CHAPTER–5

MINERAL CHEMISTRY

5.1 Introduction

A detailed description of minerals and their textural relationships within different rock types of the Makrohar granulite belt has been extensively covered in the petrography section (chapter 4). This chapter elaborates on the application of Electron Microprobe Analysis (EPMA) to portray the mineral chemistry of diverse mineral phases. The EPMA technique proves valuable as it reveals chemical variations within mineral grains and regions of chemical equilibrium. Unlike many other analytical methods that provide only bulk rock composition, EPMA enables the determination of composition at a finer scale. This is especially crucial for identifying certain minerals, such as cordierite, which closely resemble quartz and feldspar under a standard microscope. Moreover, EPMA chemical data plays a vital role in the application of different geothermobarometric models. The Electron Microprobe Analyses (EPMA) was carried out to ascertain the chemical composition of individual minerals across various rock types. Fresh rock samples from the study area were carefully chosen for EPMA analysis of different silicate minerals. The analysis focused on unaltered minerals, avoiding those that had undergone alteration. Throughout the analysis process, precautions were taken to avoid altered portions. Electron Microprobe Analyses were conducted on co-existing mineral pairs, namely garnet-biotite, garnet-cordierite-biotite-plagioclase, orthopyroxene-clinopyroxene, Garnet-clinopyroxene-plagioclase and Amphibole-plagioclase. These selections aimed to investigate cation exchanges such as Fe-Mg between garnet and biotite, orthopyroxene and clinopyroxene, garnet and clinopyroxene, as well as the interactions involving Mg,

Fe, and Al between plagioclase and amphiboles. The conditions of pressure and temperature during regional metamorphism were estimated employing various contemporary thermodynamic models. Before delving into mineralogy, the analytical methodology employed to study the rocks and minerals is thoroughly discussed below.

5.2 EPMA analytical technique

The EPMA (CAMECA SX Five) analysis was performed at the DST–SERB National Facility, Department of Geology, Centre of Advanced Study, Institute of Science,Banaras Hindu University. To prepare the sample, a thin polished section was coated with a 20 nm carbon layer using the LEICA-EM ACE200 instrument. Operating the CAMECA SX Five instrument at 15 kV and 10 nA with an aLaB6 source for electron beam generation, the positioning of crystals (SP1-TAP, SP2-LiF, SP3-LPET, SP4- TAP, and SP5-PC1) relative to corresponding wavelength dispersive (WD) spectrometers (SP#) was confirmed using the internal standard, natural silicate mineral andradite. For analysis, the following X-ray lines were utilized: F-Kα, Na-Kα, Mg-Kα, Al-Kα, Si-Kα, P-Kα, K-Kα, Cl-Kα, Ca-Kα, Ti-Kα, Cr-Kα, Mn-Kα, Fe-Kα, Ni-Kα, and Sr-Lα. Standard minerals including apatite, albite, barite, celestite, corundum, chromite, halite, hematite, orthoclase, peridotite, periclase, wollastonite, rutile, rhodonite, along with synthetic Ni metal from CAMECA AMETEK, were used for regular calibration and quantification. The processes of routine calibration, data acquisition, quantification, and data processing were conducted using Sx SAB version 6.1 and SX-Results software from CAMECA. The representative EPMA data of different minerals are presented in Tables 5.1–5.8.

5.3 Garnet

Garnet holds significant importance within metamorphic rocks due to its pivotal role in various geothermobarometry models, enabling the assessment of pressure-temperature (P-T) conditions and petrogenesis. The analysis of garnet from pelitic granulite, calc-silicate granulites, garnet-bearing gneisses, and garnetiferous amphibolites, their formula per unit calculated cations based on the 12-oxygen basis, end-member Py, Alm, Gro and Sp are are derived from AX software (Holland and Powell, 2005) given in table 5.1. The garnet structural formula is $X_3Y_2Z_3O_{12}$ (on a 12-oxygen basis), where X can be 3 ($Fe^{2+,}$ Mn, Mg, Ca), Y can be 2 (Al, Ti, Cr, Fe^{3+}), and Z is (Si_3O_{12}). Nonetheless, minor deviations exist in X (ranging from 2.93 to 3.22), Y (ranging from 1.98 to 2.15), and Z (ranging from 2.85 to 3.02) when compared to the ideal formula ($X_3Y_2Z_3O_{12}$). The chemical composition of garnet varies widely based on mineral associations, overall rock chemistry, and metamorphic conditions. An essential characteristic of garnet is its intricate crystal structure, with changes in temperature and pressure influencing the cation coordination number within the structure, resulting in its increase or decrease. Consequently, the crystalline state of garnet is indicative of its composition. Within the examined rocks, garnet primarily consists of a solid solution encompassing almandine, pyrope, grossularite, and spessartine end-members. In these studied rocks, garnet contains 24.35 to 84.86 mol% almandine, 0.34 to 17.93 mol% pyrope, 3.17 to 73.25 mol% grossularite, and 1.97 to 3.98 mol% spessartite. The pyrope content of garnet follows this trend across different rock types: Garnetiferous amphibolite> Garnet bearing gneiss > Pelitic granulites > Calc-silicate granulites and grossularite content follow this trend: Calc-silicate granulites > garnetiferous amphibolites > Pelitic granulites > Garnet bearing gneiss. The plot of the garnet compositions using the triangular (Ca+Mn)–Mg–Fe^{2+}

diagram (Figure 5.1), all garnets from Garnet bearing gneisses, pelitic granulites and garnetiferous amphibolites show higher contents of almandine and calc-silicate exhibit elevated grossartite-spessartite content. The garnets from the studied rocks, X_{Mg} vary from 0.01–0.28. This variation can be attributed to Mnor Ca, which occupy the eight-fold coordination site within the garnet crystal structure. The garnets of pelitic granulites, Garnet bearing gneiss, and garnetiferous amphibolites display relatively low CaO content, ranging from 0.9 to 7.3 wt% and the upper limit is notably observed in calc-silicate granulites, varies from 27.8 to 29.4 wt%. In garnets, manganese (Mn) content demonstrates significant variability from 0.05 to 0.12 per formula unit (p.f.u).

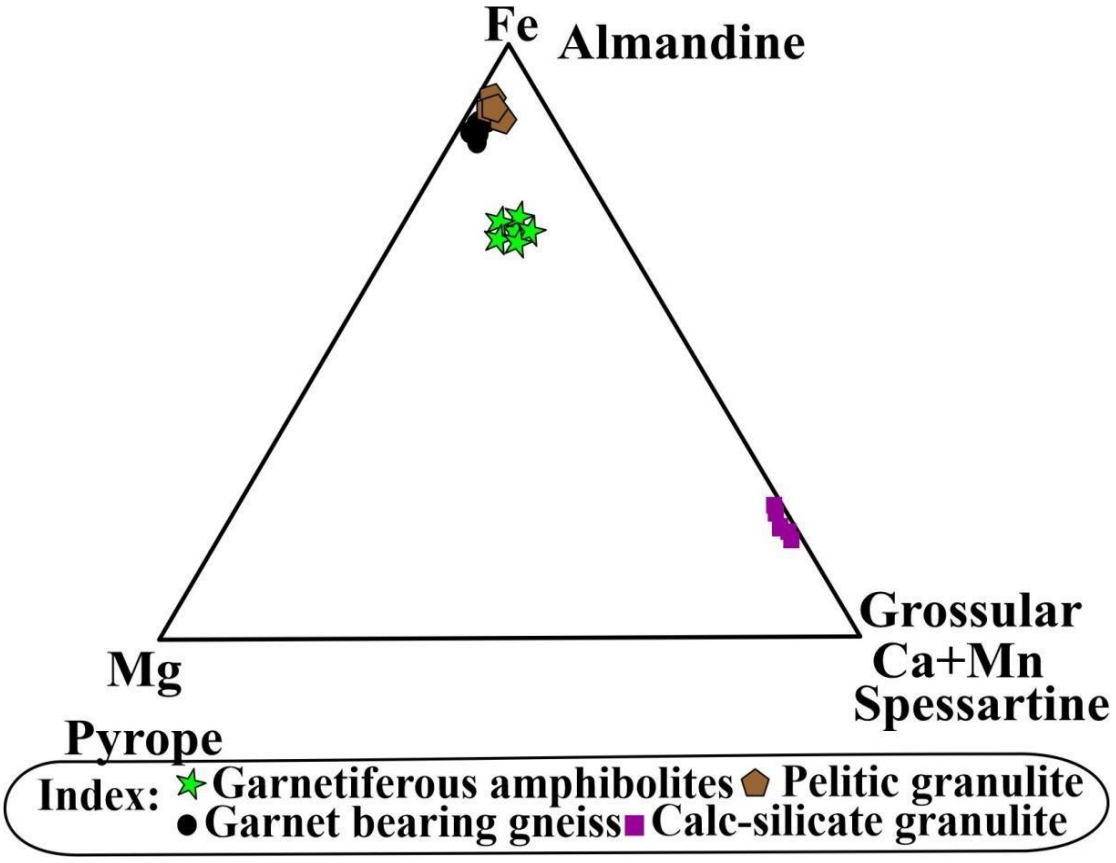

Figure 5.1 The triangular diagram showing the variation in (spessartine + grossular)–almandine–pyrope end member compositions in the garnets from different rock types.

5.4 Pyroxene

The name *pyroxene* is derived from the Greek word pyro, which means fire and xenos-*stranger* which was first introduced by Haüy (1801) It is an anhydrous single-chain silicate mineral found in igneous and metamorphic rocks. Poldervaart & Hess (1951) were the first to describe pyroxene nomenclatures based on $CaMgSi_2O_6$-$CaFeSi_2O_6$- $Mg_2Si_2O_6$-$Fe_2Si_2O_6$ (Diopside-Hedenbergite-Enstatite-Ferrosilite). Later, IMA/CNMMN (International Mineralogical Association/Commission on New Minerals and Mineral Names; Morimoto, 1988 and references therein) provided a series of recommendations and schemes for the classification and nomenclature of pyroxenes. The first pyroxene (diopside) structure was determined by Warren & Bragg (1928). They established that the pyroxene structure is linked to the SiO_4 tetrahedral by sharing of two oxygen atoms out of four in each tetrahedron, forming a single chain structure.

Cations surround this chain laterally in M1 and M2 sites. The M1 site atom lies between the apices and the M2 site at the base of the SiO_3 tetrahedral chain. Further, pyroxene can be sub-grouped based on cation participation in M1 and M2 sites, mostly depending on variable parameters such as pressure and temperature. The coordination of oxygen at the M1 site is fixed, i.e. octahedral, whereas at the M2 site, it is variable according to the cation size, for instance, Mg in six-fold coordination; and eight-fold coordination for Na-Ca.

The analysis of orthopyroxenes from mafic granulites, clinopyroxenes from mafic granulites, calc-silicate granulites and amphibolites, their formula per on calculated cations based on six oxygen basis, end-member Wo, En and Fs are derived

from mineral calculation excel sheet (Preston and Still, 2001) are given in table 5.2&5.3respectively. The recalculated formulae approximate the ideal formula: [(Mg, Al, Fe^{2+}, Mn, Ca,Ti)$_2$ (Si, Al)$_2$ O_6].

5.4.1 Orthopyroxene

The depicted triangular diagram (Fig. 5.2) shows analyzed pyroxenes. Orthopyroxene of mafic granulites aligns with clinoferrosilite composition, adjacent to hypersthene, a solid solution of Mg and Fe end members. These orthopyroxenes primarily constitute a solid solution of enstatite and ferrosilite, with En (41.95–47.5) mol%, Fs (51.07–55.42) mol%, and Wo (0.86–2.36) mol%.). An essential feature of orthopyroxene chemistry is the Al content and this may be dependent on several factors: (a) host rock composition; (b) the composition of the coexisting mineral (Binns, 1962, 1969; Leelanandam, 1967); and (c) the pressure-temperature conditions of the formation (Dobretsov, 1968). The Al_2O_3 content of the orthopyroxenes varies from 0.32–0.69 wt%. The X_{Mg} values ranging from 0.44 to 0.49 correspond to hypersthene. The calcium content of orthopyroxene (0.014–0.048 p.f.u. based on 6 oxygens) is lower than that of clinopyroxene.

5.4.2 Clinopyroxene

The coexisting clinopyroxene plot in a triangular end member $CaSiO_3$–$MgSiO_3$– $Fe^{2+}SiO_3$ diagram lies in the field of headenbergite and diopside. The X_{Mg} of clinopyroxene ranges between 0.29 and 0.70. It has higher X_{Mg} and Al content compared to orthopyroxene. Ca-content of the clinopyroxene varies between (0.86 to 1.07p.f.u) suggesting the evidence of high content of Ca in clinopyroxene, which is a characteristic of mafic granulite assemblages. The Al_2O_3 content in clinopyroxene

varies between 0.34 to 1.49 wt%. The higher amounts of Al_2O_3 present reflect an increasing Jadeite component, indicating higher pressures attained during metamorphism. The clinopyroxenes from calc-silicate granulites are mainly solid solutions of wollastonite (51.79–49.66 mol%), enstatite (14.13–15.77 mol%) and ferrosilite (33.46–35.18 mol%) (Table 5.2). The X_{Mg} value varies from 0.29 to 0.32 and the Ca content ranges between 1 and 1.07p.f.u. reflecting characteristic high Ca contentof calc-silicate granulites.

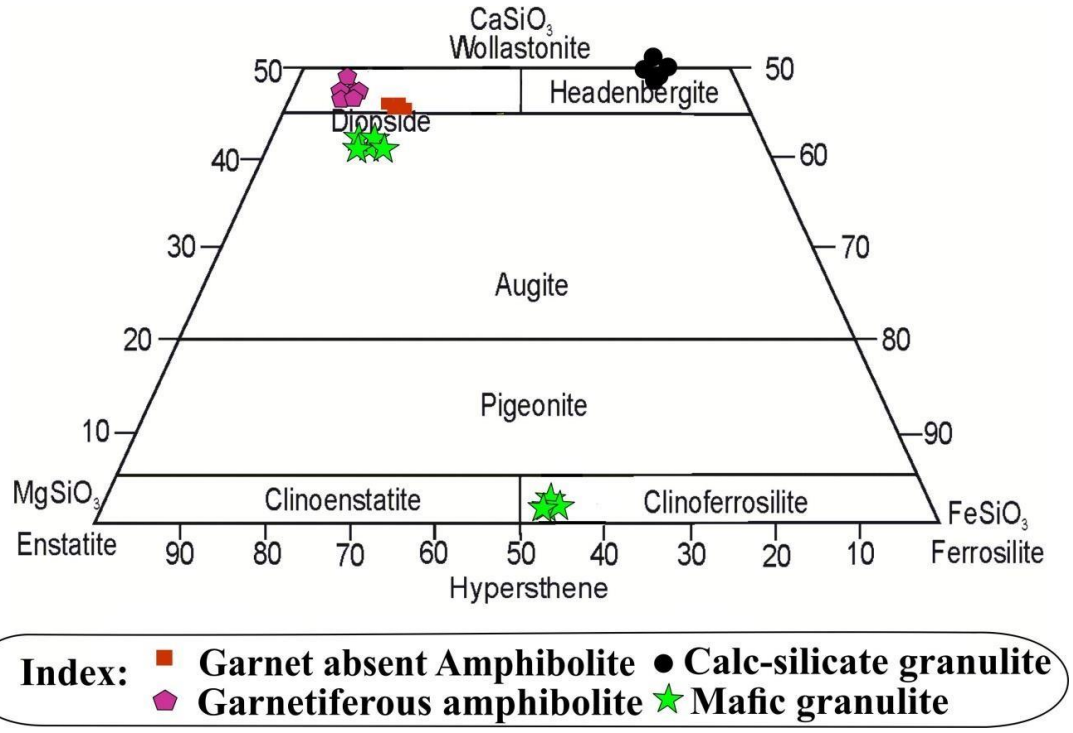

Figure 5.2 A $CaSiO_3$- $MgSiO_3$- $FeSiO_3$ composition diagram of pyroxenes showing the plot of clinopyroxenes and orthopyroxenes from different rock types.

5.5 Amphibole

The term "amphibole" stems from the Greek word for "varied" due to its diverse compositions and appearances. Amphiboles and pyroxenes are chain silicates, with essential distinctions highlighted by Schaller and Vlisidis (1961). Amphiboles feature a significant presence of hydroxyl ions, differentiating them from pyroxenes.

Amphiboles Comprising (Si, Al)O_4 tetrahedral silicates, create a double chain structure with a unit composition of Si_4O_{11}. This structure incorporates inner (T1) and outer (T2) tetrahedra along the C axis, spaced approximately 5.3Å apart. Hydroxyl ions link the hexagonal spaces formed by the double-chain silicates. The general formula of amphibole is $A_{0-1}B_2C_5T_8O_{22}$ $(OH, F)_2$ with A-site hosting large cations (Na, K), B-site for M4 cations (Ca, Na), C-site for M1, M2, M3 cations, and T-site for tetrahedral coordination (T1, T2) with $O_3(OH)$. Amphiboles are frequently encountered in both igneous and metamorphic rocks, holding potential for pressure, metamorphism and deformation measurements based on total Al content, which varies with pressure. Leake (1965) proposed criteria involving Si and Al^{VI} atoms to distinguish between igneous and metamorphic amphiboles with an upper limit on Al^{VI} in amphiboles. This limit increases with pressure, beyond which potential inaccuracies may arise. Electron microprobe analyses of amphiboles from amphibolites and mafic granulites along with their structural formulae calculated using 23 oxygen atoms, derived from mineral calculation excel sheet (Preston and Still, 2001) are presented in Table 5.4. All amphiboles from amphibolites depicted on the Leake classification diagram are located within the ferrotschermakite domain and in mafic granulites lies in magnesiohornblende and actinolite field (Fig. 5.3). The alumina content in amphibole is influenced by (a) host rock composition, particularly $Al_2O_3/(Al_2O_3 + SiO_2)$ ratio, and (b) pressure-temperature conditions. Leak et al. (1965) proposed that Al^{IV} content in amphibole increases with pressure. Amphiboles from magmatic and contact metamorphic rocks typically exhibit lower Al^{VI} and Si contents compared to those in regionally metamorphosed rocks. The Al^{IV} and Al^{VI} content of amphibole varies from 0.32 to 1.45 and 0.13 to 0.60 per formula unit

(p.f.u.), respectively.

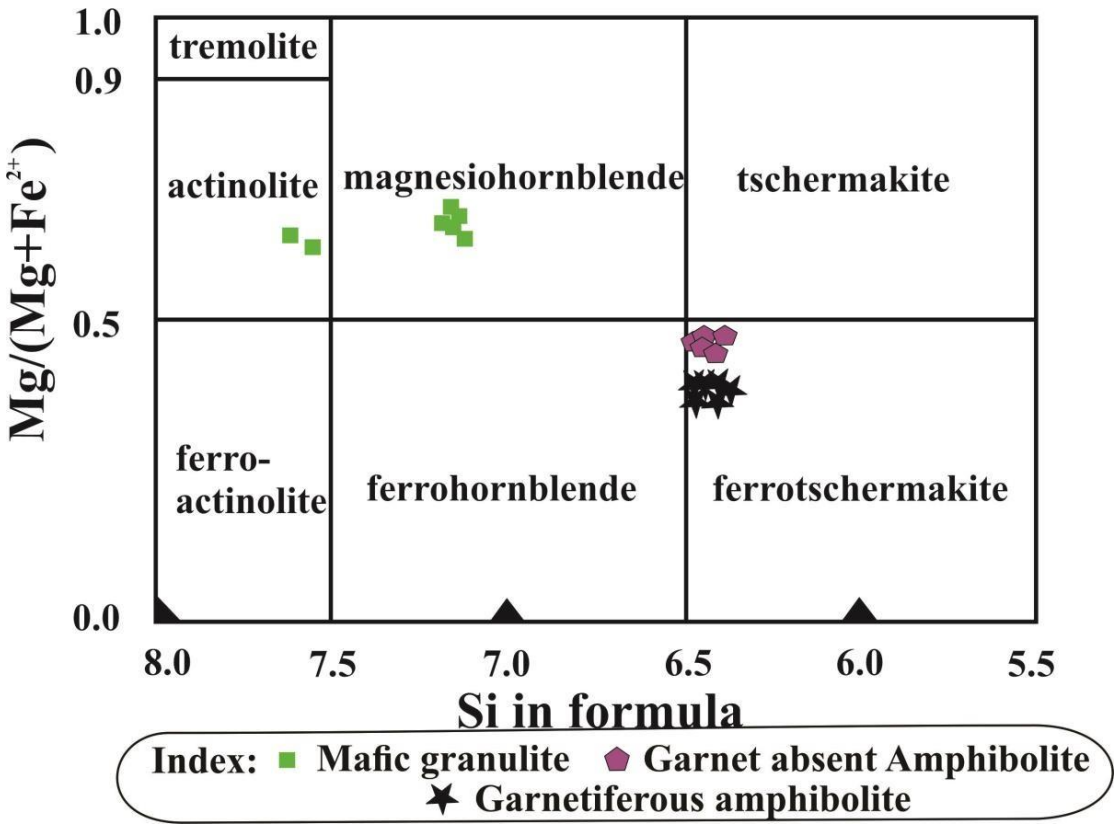

Figure 5.3 Amphibole classification diagram (after Leake et al., 1965) for the amphibolite and maficgranulite of Makrohar granulite belt.

5.6 Cordierite

Cordierite is a magnesium-iron-aluminium cyclosilicate that forms when argillaceous rocks undergo contact or regional metamorphism. The stoichiometry approximates the ideal formula: $[(Mg, Fe^{2+})_2(Al_4Si_5O_{18})nH_2O]$. Iron in the cordierite is almost always present and Mg-rich and Fe-rich cordierite show a solid solution between them. The cordierite structure accommodates molecular water with values of n commonlybetween 0.15 and 0.80 (Deer et al., 1986). The cordierite analyses show a summation between 93.83 to 96.84 wt% suggesting that it may be hydrous, containing 3.16–6.17 wt% H_2O and gaseous species as cordierite has a wide channel

site in the core of its six- membered ring structure that may hold molecular H_2O, CO_2, and to a lesser extent, other volatile molecules like CH_4, N_2, and Ar. (Schreyer & Yoder, 1964; Gibbs, 1966; Le Breton & Schreyer, 1993; Harley et al., 2002). It is now well accepted that cordierite's molecular water content is a function of P and T (Newton & Wood, 1979; Mukhopadhyay& Holdaway, 1994; Carey, 1995). Table 5.5 shows the cordierite analyses and structural formulas based on 18 oxygens.

The cordierite microprobe studies show only limited and irregular zoning indicating varied dominance of the action of small-scale cation exchange with inclusion, diffusion, and continual re-equilibration with matrix grains after nucleation. Insignificant amounts of Na_2O and K_2O are commonly present, ranging from 0.46 to 0.89 wt% and 0.04 to 0.16 wt%, respectively. The X_{Mg} varies between 0.63 and 0.66. Thompson et al. (2002) suggest that K content increases with temperature and decreases with water content. Thus, it can be inferred that the water content in cordierite will be below basedon the depletion of K in cordierite.

5.7 Mica

The mica minerals are phyllosilicates, commonly found in igneous, sedimentary and metamorphic rocks. It is mainly composed of two tetrahedral silicon sheets between which an octahedrally coordinated cation exists. An additional OH-(hydroxyl ion) is associated and completes the sandwiched octahedral cations. These octahedral cations coordination are either in the form of brucite layer $Mg_3(OH)_6$ or in gibbsite layer $Al_2(OH)_6$. Micas have the general chemical formula $X_2Y_{4-6}Z_8O_{20}(OH, F)_4$, where Xstands for K, Na, Ca, Ba, Rb, Cs; Y stands for Al, Mg, or Fe, Mn, Cr, Li; and Z stands forSi or Al but also Fe^{3+} and Ti^{4+}.

The mica group is further subdivided based on the number of Y ions present into 4 and 6 di-octahedral (muscovite) and tri-octahedral (biotite) classes, respectively. However, mica can be sub-classified as *common mica* in which K or Na are dominant ions in X, whereas if a Ca ion is present, it is known as *brittle mica*. In trioctahedral mica, the number of Y ions equals three atoms. Depending upon prevailing Physico-chemical conditions and the nature of melt, sometimes K in the X site may be replaced by Ba, Rb, or Cs; therefore, the total sum of X sites in the formula may be more than unity.

5.7.1 Biotite

The electron microprobe data of biotite from pelitic granulites, garnet-bearing gneisses and amphibolites, with their structural formula (calculated based on 11 oxygen), are presented in Table 5.6. The structural formula approximated the ideal formula of biotite: $[(K, Na, Ca)(Al^{VI}, Mg, Fe, Mn, Ti)_3(Si, Al^{IV})_4O_{10}(OH)_2]^{.2}$.

The biotite is composed of annite $[K_2Fe_6(Si_6Al_2O_{20})(OH)_4]$, siderophyllite $[K_2Fe_5Al(Si_5Al_3O_{20})(OH)_4]$, phlogopite $[K_2Mg_6(Si_6Al_2O_{20})(OH)_4]$, and eastonite $[K_2Mg_5Al(Si_5Al_3O_{20})(OH)_4]$. The biotites analyses display a wide range of X_{Mg} (0.30 to 0.69). The wide range of variation indicates the following trend of X_{Mg} in biotites; mafic granulites (0.67-0.69) > garnetiferous amphibolites (0.51 to 0.53) > garnet bearing gneisses (0.43 to 0.49) > garnet absent amphibolites (0.37-0.39) > pelitic granulites (0.30 to 0.32). The Al^{IV} content of biotites from all studied rock samples varies from 2.29 to 2.78 p.f.u.

In the triangular diagram Mg–(Fe+Mn) – Ti (Fig.5.5a), the plot of biotite lies between Mg and (Fe+Mn) line. The plot of biotites from different rocks shows a decrease of Ti with an increase of Mg, suggesting preferential substitution of Mg by Ti in the octahedral layer. In Mg – (Fe+Mn) – (Al^{IV}+Ti) (Fig.5.5b), a plot of biotite depicts the decrease of (Al^{IV}+Ti) with an increase in Mg, indicating that Al^{VI}+Ti substitutes Mg relative to Fe.

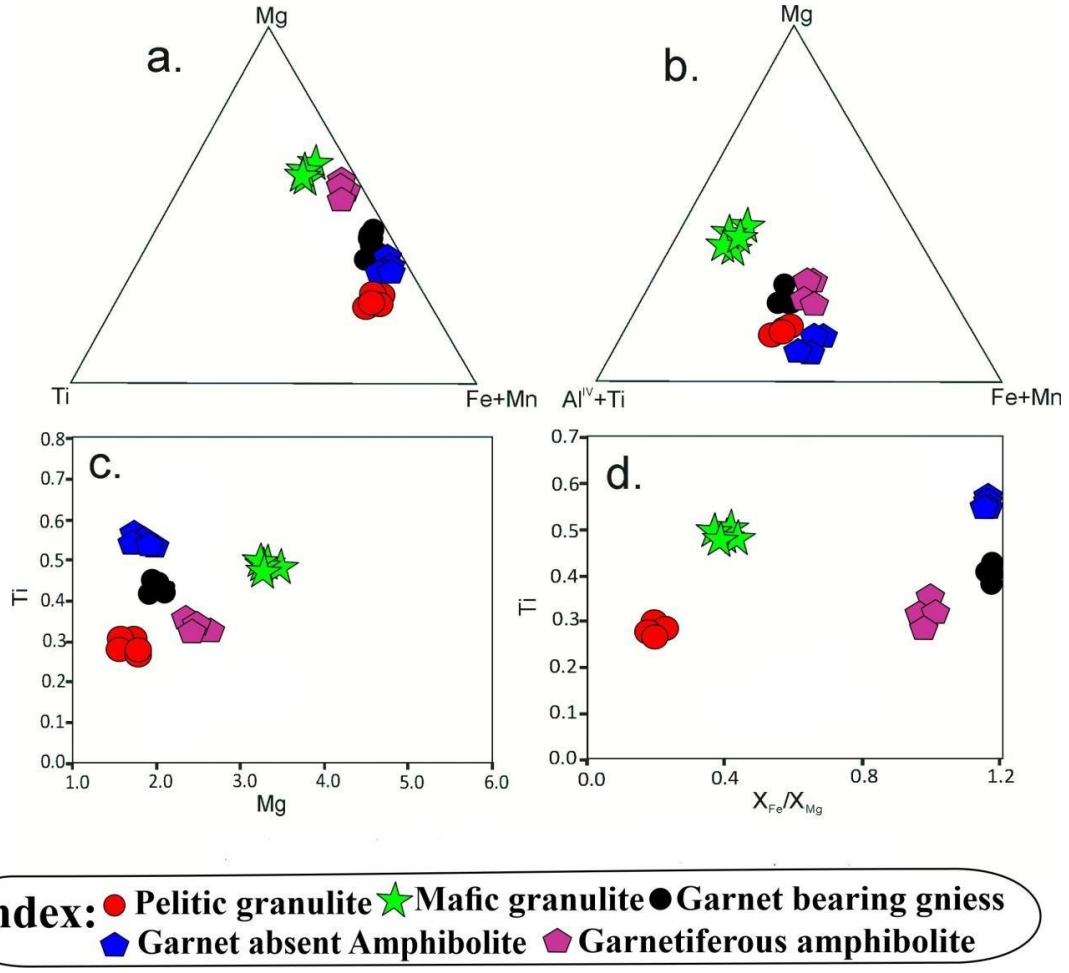

Figure 5.4 (a) A plot of microprobe analyses of biotites from different rock types in the Mg- Ti - (Fe+Mn) diagram. (b) A plot of microprobe analyses of biotites from different rock types in the Mg- (Al^{IV}+Ti) - (Fe+Mn) diagram. (c) A plot of Ti vs Mg shows a negative trend. (d) A plot of X_{Fe}/X_{Mg}vs TiO_2 shows a linear relationship.

5.7.2 TiO_2 content

The TiO_2 content of biotite is very significant in estimating the metamorphic grade of rocks (Engel & Engel, 1960; Kwak, 1968; Guidotti, 1970). In the study area, the amount of TiO_2 in biotite from the amphibolites and mafic granulites is higher than in pelitic granulite and garnet-bearing gneisses. The high content of (more than 4.5 Wt%) TiO_2 in biotite from garnet absent amphibolites, although the low content of TiO_2 in various rocks may be due to their formation, was observed during retrogression. The plots of Ti vs Mg (Fig.5.4c) and Ti vs X_{Fe}/X_{Mg} (Fig.5.4d) show a negative and linear correlation, respectively.

5.8 Feldspar

Feldspar, a diverse group of minerals, is ubiquitous in the studied litho units. It includes alkali feldspars ($NaAlSi_3O_8$–$KAlSi_3O_8$) and plagioclase feldspars ($NaAlSi_3O_8$–$CaAl_2Si_2O_8$). The triangular diagram illustrates the chemical variation in feldspar from different rock types (Fig. 5.5). Feldspar compositions from garnet-bearing gneisses and garnet-absent amphibolites are andesine, while those from mafic granulites and garnetiferous amphibolites are labradorite and pelitic granulites are Oligoclase in composition. Representative analyses and structural formulae are listed in Table 5.7.

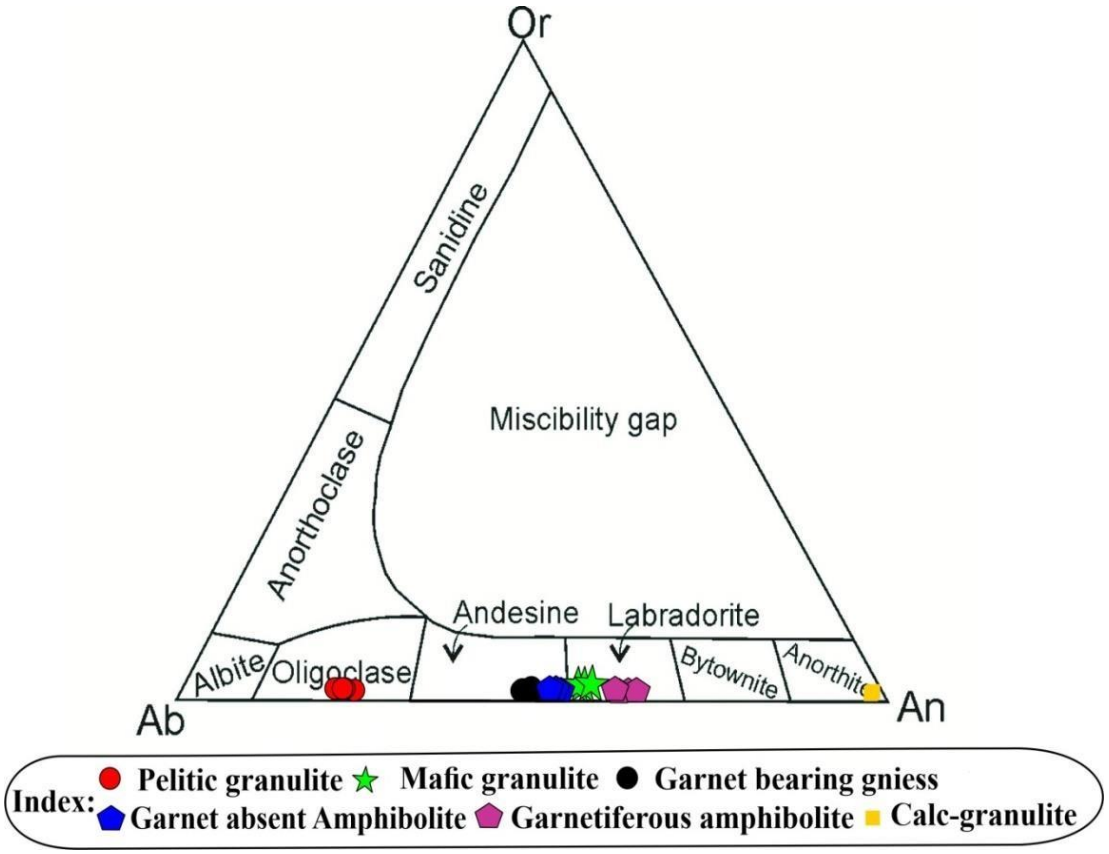

Figure 5.5 Triangular $NaAlSi_3O_8$ - $KalSi_3O_8$ - $CaAl_2Si_2O_8$ diagram showing plots of alkali feldspar and Plagioclase feldspar.

5.9 Sillimanite

The electron microprobe data of the sillimanite and their structural formulae (based on 10 oxygen) from pelitic granulites is presented in Table 5.8. The composition isrelatively pure Al_2SiO_5. The most common ion replacing aluminium in the sillimanite structure is the ferric ion, while other elements, viz. Ti and Cr are in minimum amounts. The Al-content ranges between 3.89 and 4.11 p.f.u. sillimanite includes minor amounts ofCr and Fe. The Cr and Fe content vary from 0.001 to 0.008 p.f.u. and 0.01 to 0.04 p.f.u., respectively.

5.10 Sphene, clinozoisite and Ilmenite

The electron microprobe data of the sphene, clinozoisite and ilmenite and their structural formulae are presented in Table 5.9. The structural formula of ilmenite calculated on a six-oxygen basis deviates slightly from the ideal formula due to the presence of Fe^{3+} and minor amounts of Ti, Cr, Ca and Mn. Ca- content of sphene and clinozoisite present in calc-silicate granulites vary from 1.03 to 1.07 p.f.u and 1.92 p.f.u, respectively.

5.11 Monazite dating

5.11.1 Introduction

This section employs monazite dating methods to acquire absolute ages of poly- metamorphic events of pelitic granulites (K-1) and garnet-bearing gneisses (M-1). Monazite is a minor mineral and was discovered by (Breithaupt, 1829), a curiosity that is one of the rare minerals commonly found in pegmatites. The most extensive monazite study was done by (Overstreet, 1967), which mainly consisted of thorium and rare earth elements. The large size of monazite crystals is preserved in various museums, mainly in Madagascar, the USA, Sri Lanka and Arendal (Norway). Monazite was first identified as a radioactive mineral by Marie and Pierre Curie (Curie, 1898). Since Th-U-Pb^T chemical dating was first applied in thorite and uraninite (Parslow, 1985). Monazite mineral is a phosphate of LREE [(Ce, La, Nd, Th) PO4] with abundant U, Th and little Pb (Parrish, 1990). The rapid accumulation of radiogenic lead (*Pb) is possible to a required level, analyzed with an electron probe (Montel et al. 1996). Pb diffusion is very low in the monazite under the crustal environment, whereas it presents a relatively broad and homogeneous distribution (Gardés et. al., 2007; Montel et al., 2018). Monazite dating with the help of an

electron microprobe has been performed by several researchers based on the abundance of Th, U and Pb (Williams et al., 1999; Montel et al., 1996; Suzuki and Adachi, 1991, 1994; Braun et al., 1998]. Monazite presents in several igneous, metamorphic, and diverse hydrothermal rocks as accessory minerals, and also presents in psammitic sediments and sedimentary rocks as a detritic phase (Chang et al., 1996). An uncommon existence of monazite is recognized in lunar basalts by (Lovering et al., 1974). The EPMA monazite dating technique is a reliable technique to identify the recorded history of polymetamorphic events (Bhowmik et al., 2014; Karmakar et al., 2011; Rosa- Costa et al., 2008; Prabhakar, 2013). Monazite dating and mineral chemistry are powerful features for dealing with geological problems, including the superposition of lithosphere and petrological evolution during geological history. The analysis of chemical ages and statistical calculation in monazite was discussed by (Montel et al., 1996), while (Williamset al., 1999) derived an age distribution map for the first time for a particular monazite crystal. EPMA dating technique is based on the quantification of Th, U, and Pb with appropriate accuracy and precision. Various factors like; sample preparation, instrument setup, and calibration with current intensity play a crucial role unless data treatment introduces several error types (Pyle et al., 2005; Spear et al., 2009).

5.11.2 Analytical techniques

The analytical work was performed using an electron probe microanalysis (EPMA) on a CAMECA SX five instrument at the DST-SERB National Facility, Department of Geology (CAS), Institute of Science, BHU. The thin polished section was coated with a 20 nm thin layer of carbon using a LEICA-EM ACE200 carbon coater instrument. The EPMA instrument CAMECA SX Five was operated with SX

Five software at an accelerated voltage of 15 kV and a current of 200 nA with a LaB6 source in the electron gun for electron beam generation, which is based on a new analytical protocolfor the U–Th–Pb chemical dating of monazite (Pandey et al., 2019). Andradite is used asa natural silicate mineral to verify crystal positions using an internal standard (SP2-LiF, SP3-LPET, SP4-LTAP and SP5-PET) with suitable wavelength dispersive spectrometers (SP #) using the CAMECA SX-Five instrument. The following X-ray lines were used in the analyses: F–Ka, Na–Ka, Mg–Ka, Al–Ka, Si–Ka, P–Ka, Cl–Ka, K–Ka, Ca–Ka, Ti– Ka, Cr–Ka, Mn–Ka, Fe–Ka, Ni–Ka and Ba–La. Natural mineral standards: fluorite, halite, periclase, corundum, wollastonite, apatite, orthoclase, rutile, chromite, rhodonite, hematite and barite; Ni pure metal standard was supplied by CAMECA-AMETEK which was used for routine calibration and quantification. Quantification of rare-earth element (REE) analysis in monazite mineral phases and U, Th and Y elemental X-ray mapping of monazite grains was obtained at an accelerating 20 kV voltage currents of a beam are200 nA, at 0.5 lm/pixel spatial resolution. The following X-ray lines were used in the analyses: Y–La, La–La, Ce–La, Pr–La, Nd–La, Sm–La, Eu–La, Th–Ma and U–Ma. All REE analysis was carried out on aLiF crystal attached with SP2 and Pb, Th and U were analyzed with an LPET crystal connected with the SP3 spectrometer in a CAMECA-SX five EPMA instrument. Synthetic glass standards of all REE (La to U) supplied by CAMECA AMETEK were used for routine calibration and quantification. Scanning electron microscope (SEM) analysis was performed at the DST-SERB National Facility, Department of Geology (CAS), Institute of Science, BHU. The SEM instrument was operated at an accelerated voltage of 15 kV and a current of 200 nA.

5.11.3 Sample preparation and identification of monazite

Preparation of polished thin sections has been done for petrographic investigation. The purpose of petrography is to find out the position of monazite crystals in the host mineral or matrix which helps in interpreting age. Optical microscopes have a low resolution for identifying monazite, so SEM plays an essential role in detecting monazite. Monazite occurs as an accessory phase in the rocks. Zircon causes some confusion with monazite to identify monazite grains under a petrological microscope. Monazite andzircon have some important diagnostic features and can be distinguished by their characteristics (Montel et al., 1996). In zircon crystals have a double pyramid prismatic while monazite crystals have a single pyramid. Zircons have a distinctive 0º extinction angle and coarse cleavage, while monazite has a 5-10º extinction angle. Zircons have a higher refractive index than monazite. Monazite forms rounded, subrounded, and anhedral shapes while zircon forms prisms and euhedral shapes. Pleochroic haloes of zircon are small, while monazite produces larger ones due to the abundance of Thorium. However, solely on optical properties, monazite and zircon grains cannot be easily distinguished. The SEM and energy dispersive system (EDS) are authentic instrumentsfor the immediate identification of monazite grains. Deprived of EDS, monazite can be recognized in BSE images because it is exceptionally bright (higher atomic number), even higher than that of zircon, leaving only thorite and uraninite (Montel et al., 1996). The back-scattered electron (BSE) images were used to identify the monazite grainsfrom the matrix and garnet. Some separated monazites are also used for mounting on the epoxy resin. The electron microprobe quickly detects the separated mineral through a Th-intensity signal. This method's disadvantage is the inability to find the petrographic position of dated crystals, and small crystals (<20–50 µm) are omitted during this separation process.

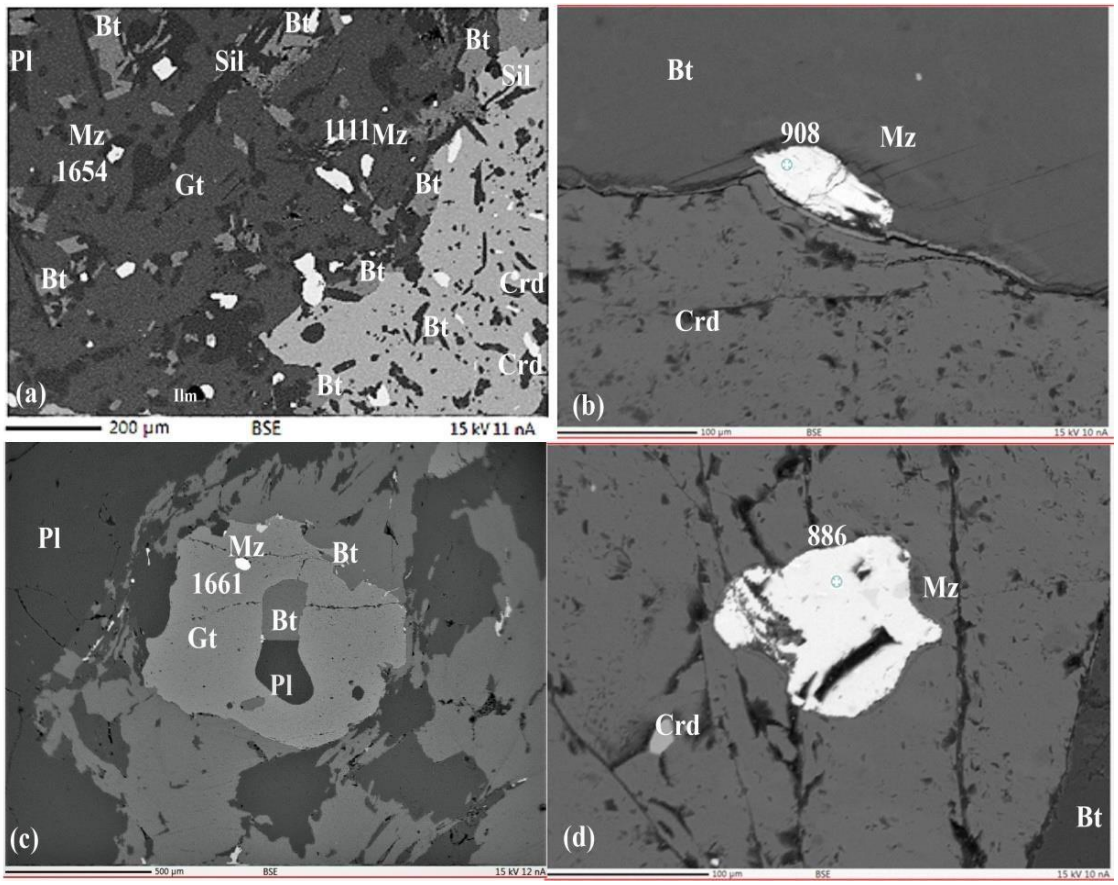

Figure 5.6 Back Scattered Electron (BSE) images are showing the microstructural and textural settings of monazite occurrences in the garnet-bearing gneiss and pelitic granulites of the study area. (a) BSE image of showing monazite inclusion in garnet of pelitic granulites. (b) Monazite grain occurs as an inclusion in cordierite as well as biotite. (c) Monazite occurs as inclusion in the garnet. (d) Monazite occurs as inclusion in cordierite rim.

5.11.4 Electron microprobe dating

Pelitic granulites (K-1) and garnet-bearing gneisses (M-1) were taken from the Kumiya and Piprakurund area for U-Th-Pb^T monazite dating. We selected 20 monazite grains from the samples after through scanning electron microscopic imaging and textural interpretation yielding 33 geocronological data. The structural formulae and mineral chemistry of monazite grains as well as their associated geochronological age with an error are shown in table 5.10. The analyzed monazite grains are incorporated within porphyroblastic garnet, cordierite, biotite, and matrix (Fig.5.6). Monazite grains at the core of the garnet produced older ages and many

monazite grains embedded in the periphery zone produced younger ages in pelitic granulites (Fig.5.6a). Garnet is rimmed by cordierite and exhibits a corona texture (Fig.5.6a) consisting of biotite, sillimanite and quartz as inclusion that leads to cordierite formation. Monazite grains are also present in the cordierite, biotite (Fig.5.6b-d), which provide younger age. Monazite occurs as inclusion in the garnet shows late Peleoproterozoic age this indicate the peak metamorphism stage (Fig. 5.6c). Monazite occurs as inclusion in the cordierite shows Neoproterozicage this indicate the postpeak metamorphism stage (Fig. 5.6d). The monazite grains contain 3.156– 11.864 wt% of thorium oxide (ThO_2), 0.112–0.730 wt% of uranium oxide (UO_2) and 1.07– 0.161 wt% of lead oxide (PbO) in the pelitic granulite sample (K-1). The garnet-bearing gneiss sample (M-1) contains 5.424–8.769 wt% of ThO_2, 0.288–1.053 wt% of UO_2 and 0.017–0.608 wt% of (PbO). The normalized cations based on the four oxygen basis are presented in Table 5.10. In BSE-SEM images, monazite grains are xenomorphic to subidiomorphic in shape and their size ranges from small to medium (10-60 μm) (Fig. 5.7). The BSE-SEM images of the monazite grains show no zoning and are homogeneous in composition (Fig. 5.7). The un-zoned monazite grains make it difficult to interpret various age domains related to their metamorphic stages. However, the distribution and petrographical association of monazite grains withindifferent minerals play a significant role in interpreting the various age domains and their corresponding metamorphic events.

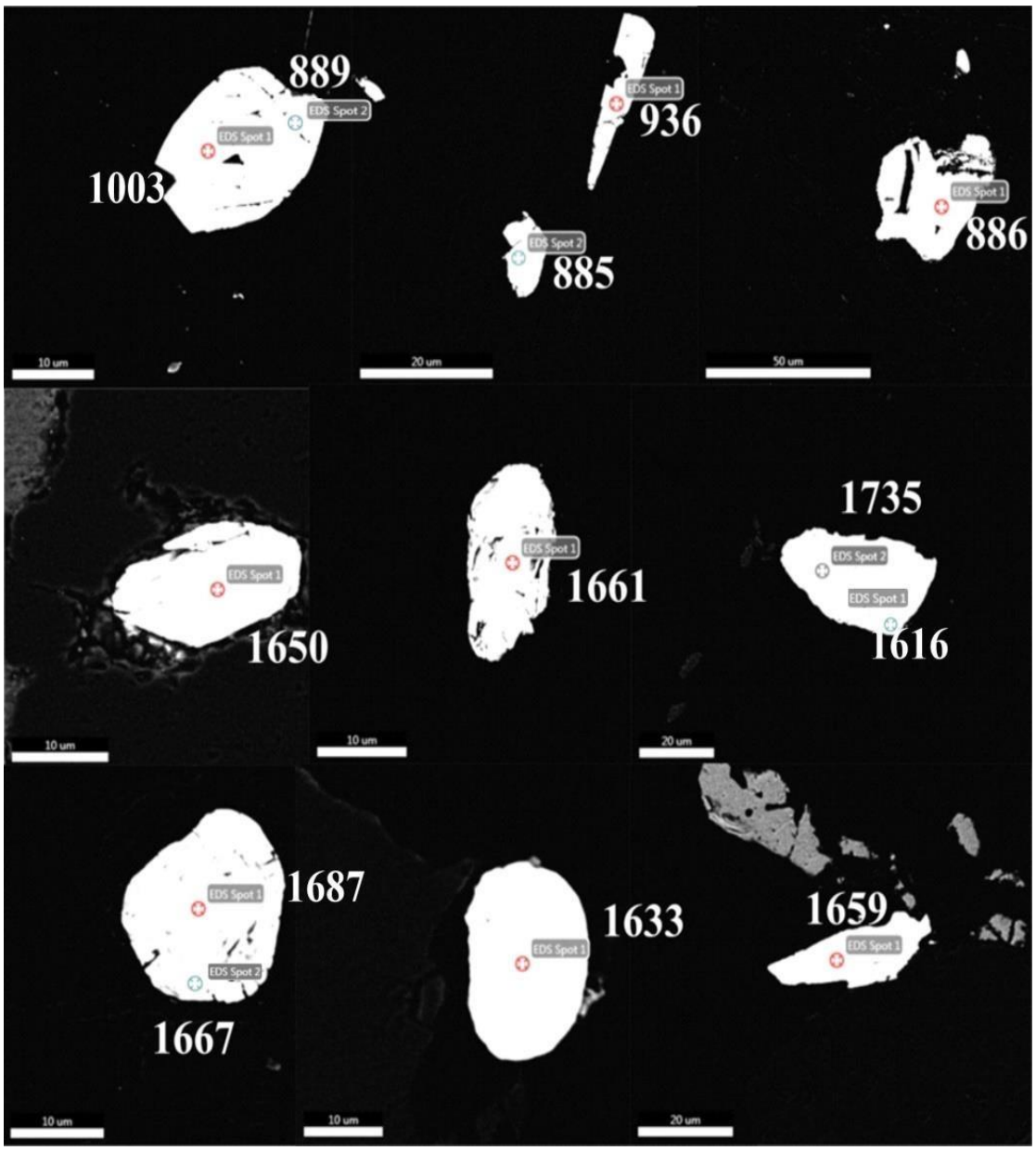

Figure 5.7 BSE-SEM images of monazite grains of Pelitic granulites and garnet bearing gneisses.

The electron microprobe analysis of monazite grains show that the geochronological ages of the studied rock samples range from the late Paleoproterozoic to Neoproterozoic period, with older ages found in the cores and younger age in the rims of the monazite grains respectively (Fig. 5.7). EPMA dating has generated two age domains, and the calculated monazite age range is from 1529 to 1743 Ma and 874 to 1111 Ma from K-1, while 822 to 1014 Ma ages are preserved

in M-1 samples. The Weighted mean age distributions and probability–density ages of Pelitic granulite (K-1) and garnet-bearing gneiss (M-1) are plotted using the Isoplot program (Ludwig, 2003) and are shown in (Fig 5.8). The estimated Weighted mean age 1655 ± 30 Ma (n = 14, MSWD = 4.3) represents a peak metamorphic event and the Weighted mean age 910 ± 31 Ma (n = 19, MSWD = 9.3) represents a post peak metamorphic event. The electron microprobe dating of monazite grains has generated a two-age domain from pelitic granulite rocks, which lies around the late Paleoproterozoic and Neoproterozoic ages and garnet-bearing gneisses represent Neoproterozic ages.

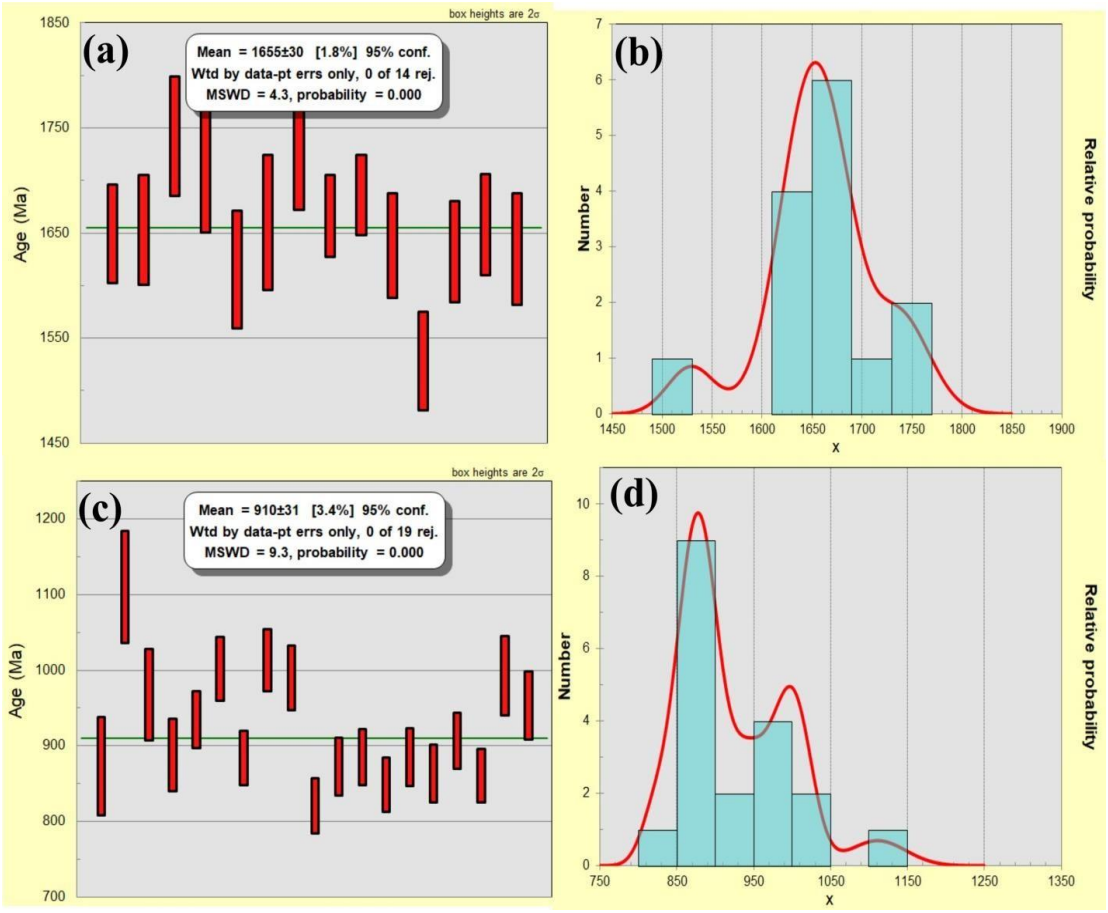

Figure 5.8(a) and (b) Weighted-average ages and probability density ages of pelitic granulite showing older age, (c) and (d) Weighted-average ages and probability density ages of pelitic granulite and garnet-bearing gneiss sample showing younger age.

Table 5.1 Chemical analysis and structural formulae (based on 12 Oxygen) of garnet from peliticgranulites.

Sample	**K-1**									
Domain	101-r	102-c	103-c	104-r	107-r	109-r	110-c	111-c	113-r	114-c
SiO_2	35.87	37.01	36.19	36.74	36.72	35.94	36.19	35.59	37.01	37.35
TiO_2	bdl	0.12	bdl	bdl	0.12	bdl	bdl	0.06	0.12	bdl
Al_2O_3	20.3	21.31	20.37	20.48	21.07	20.21	20.37	21.18	21.31	21.55
Cr_2O_3	0.08	0.06	0.11	0.06	0.08	0.07	0.11	0.09	0.06	0.07
FeO	38.15	36.65	37.54	35.73	37.1	38.28	37.54	37.59	36.38	36.03
MnO	1.13	1.55	1.46	1.34	1.33	1.18	1.46	1.39	1.7	1.42
MgO	2.02	1.87	2.29	2.31	1.86	2.05	2.29	2.23	1.87	2.21
CaO	1.61	1.43	1.49	1.31	1.58	1.59	1.49	1.18	1.43	1.11
Total	**99.16**	**100**	**99.45**	**97.96**	**99.85**	**99.21**	**99.45**	**99.32**	**99.88**	**99.72**
Si	2.944	2.996	2.956	3.028	2.985	2.94	2.971	2.965	2.993	2.994
Al^{IV}	bdl	bdl	bdl	bdl	bdl	bdl	bdl	bdl	0.007	bdl
ΣZ	2.944	2.996	2.956	3.028	2.985	2.94	2.971	2.965	2.993	2.994
Al^{VI}	1.964	2.034	1.962	1.989	2.016	1.958	1.971	2.018	2.031	2.036
Ti	bdl	0.007	bdl	bdl	0.007	bdl	bdl	bdl	0.007	bdl
Cr	0.005	0.004	0.007	0.004	0.005	0.005	0.007	0.006	bdl	bdl
Fe^{3+}	0.142	bdl	0.119	bdl	bdl	0.0139	0.051	0.037	bdl	bdl
ΣY	2.111	2.045	2.088	1.993	2.028	1.9769	2.029	2.061	2.038	2.036
Fe^{2+}	2.572	2.481	2.446	2.463	2.523	2.578	2.527	2.559	2.481	2.483
Mn	0.079	0.106	0.101	0.094	0.092	0.08	0.102	0.1	0.117	0.109
Mg	0.247	0.225	0.279	0.283	0.225	0.251	0.281	0.282	0.225	0.263
Ca	0.142	0.124	0.13	0.114	0.137	0.138	0.131	0.107	0.124	0.094
ΣX	3.04	2.936	2.956	2.954	2.977	3.047	3.041	3.048	2.947	2.949
X_{Mg}	**0.09**	**0.08**	**0.1**	**0.1**	**0.08**	**0.08**	**0.09**	**0.1**	**0.08**	**0.1**
Py	8	7.7	9.1	9.6	7.6	8	9.1	8.9	7.7	9.2
Alm	84.9	84.5	83.4	83.4	84.7	84.9	83.4	84.5	84.1	84.2
Gro	4.6	4.2	4.2	3.9	4.6	4.6	4.2	3.4	4.2	3.3
Sp	2.5	3.6	3.3	3.2	3.1	2.5	3.3	3.2	4	3.4

X_{Mg} = $Mg/(Fe^{2+}+Mg)$; bdl = Below Detection Limit; FeO as Total Iron

Table 5.1 contd. (from garnet bearing gneisses)

Sample	**M-1**									
Domain	11-c	12-r	14-c	15-r	17-c	18-r	19-c	20-r	25-c	24-r
SiO_2	35.43	36.85	35.18	37.08	34.13	34.5	37.18	35.73	36.62	36.72
TiO_2	bdl	bdl	bdl	bdl	bdl	bdl	bdl	bdl	0.1	0.12
Al_2O_3	20.74	20.9	20.77	21.16	20.64	21.79	21.05	20.7	20.06	20.02
Cr_2O_3	bdl	0.07	bdl	0.07	bdl	0.12	0.14	0.09	0.15	0.11
FeO	36.7	37.03	36.02	36.23	36.7	35.38	36.25	37.56	37.09	36.59
MnO	0.84	1.41	1.19	1.37	1.84	1.14	1.21	1.5	1.15	0.95
MgO	3.02	2.6	3.82	2.54	3.22	3.61	2.54	2.48	2.9	2.97
CaO	1.53	1.1	1.76	1.22	1.53	1.54	1.08	0.9	1.15	1.2
Total	**98.26**	**99.96**	**98.74**	**99.67**	**98.06**	**98.19**	**99.47**	**98.97**	**99.22**	**98.68**
Si	2.931	2.99	2.896	2.985	2.855	2.847	3.005	2.946	2.998	3.013
Al^{IV}	bdl	bdl	bdl	bdl	bdl	bdl	bdl	bdl	bdl	bdl
ΣZ	2.931	2.99	2.896	2.985	2.855	2.847	3.005	2.946	2.998	3.013
Al^{VI}	2.022	2.039	2.015	2.008	2.035	2.119	2.03	2.012	1.936	1.936
Ti	bdl	bdl	bdl	bdl	bdl	0.007	bdl	bdl	0.006	0.007
Cr	bdl	0.004	bdl	0.005	bdl	0.008	0.009	0.006	0.01	0.007
Fe^{3+}	0.047	bdl	0.089	0.002	0.11	0.019	bdl	0.036	0.051	0.037
ΣY	2.069	2.044	2.104	2.015	2.145	2.153	2.039	2.054	2.002	1.987
Fe^{2+}	2.492	2.447	2.39	2.505	2.458	2.423	2.458	2.555	2.489	2.474
Mn	0.059	0.108	0.083	0.093	0.13	0.08	0.082	0.105	0.08	0.066
Mg	0.372	0.306	0.469	0.305	0.401	0.444	0.301	0.305	0.354	0.363
Ca	0.136	0.093	0.155	0.106	0.137	0.136	0.092	0.08	0.101	0.105
ΣX	3.058	2.954	3.097	3.008	3.127	3.083	2.933	3.045	3.023	3.008
X_{Mg}	**0.13**	**0.11**	**0.16**	**0.1**	**0.14**	**0.15**	**0.1**	**0.1**	**0.12**	**0.13**
Py	12	10.4	14.7	10.4	12.4	14.3	10.4	9.9	11.5	11.9
Alm	81.7	83.2	77.8	82.9	79.3	78.7	83.5	84.1	82.6	82.4
Gro	4.4	3.2	4.9	3.6	4.2	4.4	3.2	2.6	3.3	3.5
Sp	1.9	3.2	2.6	3.2	4	2.6	2.8	3.4	2.6	2.2

X_{Mg} = Mg/(Fe^{2+}+Mg); bdl = Below Detection Limit; FeO as Total Iron

Table 5.1 contd. (from garnetiferous amphibolites)

Sample	**S-9**									
Domain	17-c	19-c	22-c	23-r	25-c	28-c	30-c	31-r	35	39
SiO2	36.11	35.99	36.12	35.44	36.55	36.74	36.62	36.43	36.77	36.47
TiO2	bdl	bdl	bdl	bdl	bdl	bdl	0.1	0.1	0.16	bdl
Al2O3	21.73	22.36	21.67	22.1	21.16	20.92	21.06	21.1	21.62	22.21
Cr2O3	0.08	0.1	0.05	0.12	0.08	0.08	0.15	0.15	0.13	0.1
FeO	28.73	27.96	28.26	28.39	27.74	28.78	28.09	28.42	28.18	27.98
MnO	1.41	1.08	1.46	1.56	1.41	1.34	1.15	1.06	0.89	0.93
MgO	4.45	3.95	4.46	3.82	4.48	4.72	3.9	4.68	4.15	4.1
CaO	7.11	6.97	6.98	7.52	7.3	6.57	7.15	6.13	7.19	7.68
Total	**99.62**	**98.41**	**99.02**	**98.94**	**98.74**	**99.14**	**98.22**	**98.07**	**99.07**	**99.47**
Si	2.885	2.893	2.897	2.856	2.933	2.942	2.953	2.94	2.935	2.901
AlIV	bdl	bdl	bdl	bdl	bdl	bdl	bdl	bdl	bdl	bdl
ΣZ	2.885	2.893	2.897	2.856	2.933	2.942	2.953	2.94	2.935	2.901
AlVI	2.046	2.119	2.049	2.099	2.002	1.975	2.002	2.007	2.034	2.083
Ti	bdl	bdl	bdl	bdl	bdl	bdl	0.006	0.006	0.009	bdl
Cr	bdl	0.006	bdl	0.007	0.005	bdl	0.009	0.009	0.008	0.006
Fe^{3+}	0.064	bdl	0.051	0.038	0.059	0.078	0.01	0.02	0.01	bdl
ΣY	2.11	2.125	2.1	2.144	2.067	2.053	2.027	2.043	2.061	2.089
Fe^{2+}	1.855	1.88	1.845	1.876	1.803	1.85	1.895	1.918	1.881	1.861
Mn	0.095	0.073	0.099	0.107	0.096	0.091	0.078	0.073	0.06	0.063
Mg	0.53	0.473	0.534	0.459	0.536	0.564	0.469	0.563	0.493	0.487
Ca	0.608	0.6	0.6	0.649	0.628	0.564	0.618	0.53	0.615	0.654
ΣX	3.089	3.026	3.077	3.091	3.063	3.068	3.061	3.083	3.049	3.065
X_{Mg}	**0.22**	**0.2**	**0.22**	**0.2**	**0.23**	**0.23**	**0.2**	**0.23**	**0.21**	**0.21**
Py	16.8	15.6	17.1	14.7	17.2	17.9	15.3	18.3	16.2	15.9
Alm	60.9	62.1	60.6	61.2	59.6	61.3	61.9	62.2	61.7	60.7
Gro	19.3	19.8	19.2	20.7	20.1	17.9	20.2	17.2	20.2	21.4
Sp	3	2.4	3.2	3.4	3.1	2.9	2.6	2.4	2	2

X_{Mg} = Mg/(Fe^{2+}+Mg); bdl = Below Detection Limit

Table 5.1 contd. (from calc-silicate granulites)

Sample	**M-7**									
Domain	23-c	24-r	26-c	28-r	29-c	31-c	32-r	35	38	40
SiO_2	37.12	36.96	37.85	37.57	38.46	37.38	36.12	36.93	37.25	37.1
TiO_2	0.24	0.16	0.16	0.18	0.19	0.07	0.14	0.12	0.23	0.17
Al_2O_3	18.89	18.39	17.8	18.06	19.05	20.67	18.21	18.84	19.02	18.93
Cr_2O_3	0.09	0.09	0.05	0.11	0.05	0.05	0.05	0.07	0.14	0.09
FeO	12.53	13.66	13.34	13.45	12.16	12.68	13.63	13.84	13.29	13.34
MnO	0.78	1.31	1.36	1.11	1.26	1.33	1.39	1.42	1.15	1.23
MgO	0.19	0.15	0.18	0.2	0.17	0.12	0.21	0.1	0.22	0.34
CaO	29.2	28.91	28.93	28.59	28.25	27.8	29.4	28.42	28.62	28.75
Total	**99.04**	**99.63**	**99.67**	**99.27**	**99.59**	**100.1**	**99.15**	**99.74**	**99.92**	**99.95**
Si	2.954	2.947	3.007	2.994	3.022	2.932	2.907	2.938	2.946	2.938
Al^{IV}	bdl	bdl	bdl	bdl	bdl	bdl	bdl	bdl	bdl	bdl
ΣZ	2.954	2.947	3.007	2.994	3.022	2.932	2.907	2.938	2.946	2.938
Al^{VI}	1.772	1.728	1.667	1.696	1.764	1.911	1.728	1.767	1.773	1.767
Ti	0.014	0.01	0.01	0.011	0.011	bdl	0.008	0.007	0.014	0.01
Cr	0.006	0.006	bdl	bdl	bdl	bdl	bdl	bdl	0.009	0.006
Fe^{3+}	0.255	0.31	0.313	0.292	0.199	0.15	0.354	0.283	0.258	0.28
ΣY	2.046	2.053	1.99	1.999	1.975	2.061	2.09	2.057	2.054	2.062
Fe^{2+}	0.579	0.601	0.573	0.604	0.6	0.682	0.564	0.638	0.621	0.604
Mn	0.053	0.088	0.092	0.075	0.084	0.088	0.095	0.096	0.077	0.083
Mg	0.023	0.018	0.021	0.024	0.02	0.01	0.025	0.012	0.026	0.04
Ca	2.489	2.47	2.463	2.441	2.379	2.336	2.535	2.423	2.425	2.439
ΣX	3.143	3.177	3.148	3.144	3.083	3.117	3.219	3.169	3.149	3.166
X_{Mg}	**0.03**	**0.02**	**0.02**	**0.03**	**0.02**	**0**	**0.027**	**0.01**	**0.03**	**0.04**
Py	0.7	0.5	0.6	0.7	0.6	0.4	0.7	0.3	0.8	1.2
Alm	24.5	26.1	25.6	26.1	24.4	25.4	25.7	26.7	25.8	25.6
Gro	73.3	70.8	71.1	71	72.5	71.4	71	70.2	71.2	70.8
Sp	1.5	2.5	2.6	2.2	2.6	2.7	2.7	2.8	2.3	2.4

X_{Mg} = $Mg/(Fe^{2+}+Mg)$; bdl = Below Detection Limit

Table 5.2 Chemical analysis and structural formulae (based on 6 Oxygen) of Orthopyroxene from maficgranulites.

Sample	**M-13**									
Domain	36-c	38-r	40-c	41-r	43	44	46	49	51	52
SiO_2	51.89	50.26	49.16	50.5	50.24	51.42	51.63	51.91	51.57	51.45
TiO_2	0.15	0.1	0.39	0.2	0.05	0.07	0.04	0.046	0.063	0.071
Al_2O_3	0.69	0.19	0.39	0.54	0.65	0.32	0.67	0.41	0.62	0.38
FeO	29.45	32.49	32.67	32.07	29.59	29.36	30.16	30.28	30.4	30.73
MnO	0.91	1.01	1.28	0.89	1.27	0.84	0.57	0.62	0.95	0.92
MgO	15.44	15.21	14.34	15.22	15.78	15.22	15.94	14.87	14.98	15.14
CaO	1.18	0.41	1.25	0.1	0.125	0.351	0.876	0.93	1.21	0.742
Na_2O	0.07	bdl	0.03	bdl	0.06	0.02	0.07	0.02	bdl	0.01
K2O	0.01	0.03	0.01	bdl	bdl	0.04	0.02	bdl	0.01	bdl
Total	**99.79**	**99.7**	**99.52**	**99.52**	**97.77**	**97.64**	**99.98**	**99.09**	**99.81**	**99.44**
Si	2.009	1.982	1.957	1.985	1.993	2.031	1.999	2.027	2.007	2.009
Al^{IV}	bdl	0.018	0.043	0.015	0.007	bdl	0.001	bdl	bdl	bdl
Ti	0.004	0.003	0.012	0.006	0.001	0.002	0.001	0.001	0.002	0.002
Al^{VI}	0.041	bdl	bdl	0.011	0.024	0.046	0.029	0.046	0.035	0.027
Fe^{3+}	0.027	bdl	bdl	0.004	0.008	0.041	0.013	0.037	0.023	0.021
Fe^{2+}	0.927	1.071	1.087	1.051	0.974	0.929	0.963	0.952	0.966	0.982
Mn	0.031	0.034	0.043	0.03	0.043	0.028	0.019	0.021	0.031	0.03
Mg	0.891	0.894	0.851	0.892	0.933	0.896	0.921	0.865	0.869	0.881
Ca	0.049	0.017	0.053	0.004	0.005	0.015	0.036	0.039	0.05	0.031
Na	0.005	bdl	0.002	bdl	0.005	0.002	0.005	0.002	bdl	0.001
K	bdl	0.002	0.001	bdl	bdl	0.002	0.001	bdl	0.001	bdl
Total	3.982	4.021	4.049	3.996	3.992	3.992	3.988	3.99	3.984	3.985
Wo	2.5	0.9	2.6	0.2	0.3	0.8	1.9	2	2.6	1.6
En	46.2	44.4	42	45	47.5	46.7	47.1	45	44.7	45.2
Fs	51.3	54.7	55.4	54.8	52.2	52.5	51.1	53	52.7	53.2
X_{Mg}	**0.49**	**0.45**	**0.44**	**0.46**	**0.49**	**0.49**	**0.49**	**0.48**	**0.47**	**0.47**

X_{Mg} = Mg/(Fe^{2+}+Mg); bdl = Below Detection Limit; Fe^{+3} = (2* Number of oxygen)*(1-(4/cation Total)

Table 5.3 Chemical analysis and structural formulae (based on 6 Oxygen) of Clinopyroxene from maficgranulite and amphibolites.

Sample	**M-13**					**S-9**				
Domain	8	11	21	22	28	32	33	36	38	39
SiO_2	50.34	51.07	50.88	51.24	50.49	51.36	51.25	51.42	51.83	51.4
TiO_2	0.25	0.38	0.28	0.22	0.34	0.07	0.05	0.12	0.16	0.09
Al_2O_3	0.97	1.12	1.49	1.17	1.35	0.85	0.98	1.34	1.07	0.94
Cr_2O_3	0.15	0.15	0.09	0.13	0.17	0.12	0.05	0.01	bdl	0.07
FeO	12.79	12.67	12.24	12.52	12.84	10.23	10.05	9.95	10.23	10.025
MnO	0.57	0.38	0.32	0.42	0.62	0.07	0.1	0.05	0.01	0.03
MgO	12.23	12.25	12.49	12.53	12.87	13.04	13.16	12.92	13.24	12.84
CaO	21.64	21.18	21.36	20.95	21.07	23.13	23.41	23.78	23.15	23.65
Na_2O	0.15	0.16	0.16	0.15	0.21	0.14	0.08	0.13	0.04	0.18
K_2O	0.02	0.02	0.02	0.01	bdl	bdl	bdl	bdl	bdl	bdl
Total	**99.11**	**99.38**	**99.33**	**99.34**	**99.96**	**99.01**	**99.13**	**99.72**	**99.73**	**99.23**
Si	1.94	1.953	1.943	1.957	1.926	1.957	1.951	1.945	1.957	1.955
Al	0.044	0.05	0.067	0.053	0.061	0.038	0.044	0.06	0.048	0.042
Cr	0.005	0.005	0.003	0.004	0.005	0.004	0.002	bdl	bdl	0.002
Ti	0.007	0.011	0.008	0.006	0.01	0.002	0.001	0.003	0.005	0.003
Fe^{+3}	bdl	bdl	bdl	bdl	bdl	bdl	bdl	bdl	bdl	bdl
Fe^{+2}	0.412	0.405	0.391	0.4	0.41	0.326	0.32	0.315	0.323	0.319
Mn	0.019	0.012	0.01	0.014	0.02	0.002	0.003	0.002	0	0.001
Mg	0.702	0.698	0.711	0.713	0.732	0.741	0.747	0.728	0.745	0.728
Ca	0.894	0.868	0.874	0.857	0.861	0.945	0.955	0.964	0.936	0.964
Na	0.011	0.012	0.012	0.011	0.016	0.01	0.006	0.01	0.003	0.013
K	0.001	0.001	0.001	bdl	bdl	bdl	bdl	bdl	bdl	bdl
Total	4.035	4.015	4.02	4.014	4.039	4.025	4.028	4.026	4.016	4.027
Wo	44.2	43.8	44	43.2	42.7	46.9	47.2	48	46.7	48
En	34.7	35.2	35.8	36	36.3	36.8	36.9	36.3	37.2	36.2
Fs	21.1	21	20.1	20.8	21.1	16.2	15.9	15.7	16.1	15.8
X_{Mg}	**0.63**	**0.63**	**0.65**	**0.64**	**0.64**	**0.69**	**0.7**	**0.7**	**0.7**	**0.7**

X_{Mg} = $Mg/(Fe^{2+}+Mg)$; bdl = Below Detection Limit

Table 5.3 contd. (from amphibolites)

Sample	**S-13**					**S-14**				
Domain	6	8	9	11	17	18	22	23	26	29
SiO_2	51.45	51.63	51.36	51.42	51.14	51.84	51.13	50.87	51.52	51.64
TiO_2	0.08	0.14	0.16	0.12	0.11	0.08	0.07	0.15	0.1	0.09
Al_2O_3	0.5	0.88	0.42	0.34	0.68	0.59	0.92	1.01	0.57	0.49
Cr_2O_3	0.08	0.1	0.03	0.02	0.07	bdl	0.02	bdl	0.01	bdl
FeO	12.4	13.05	12.95	13.66	12.84	14.76	14.84	14.9	14.94	14.83
MnO	0.4	0.53	0.65	0.28	0.345	0.59	0.53	0.64	0.61	0.38
MgO	10.45	9.78	10.55	10.17	10.22	9.36	9.94	9.6	9.7	9.61
CaO	23.65	23.54	22.81	23.04	23.84	21.96	21.68	21.72	21.89	21.76
Na_2O	0.2	0.17	0.15	0.08	0.05	0.18	0.28	0.25	0.27	0.31
K_2O	0.5	0.04	0.01	bdl	0.04	0.15	0.01	0.11	0.08	0.03
Total	**99.71**	**99.86**	**99.08**	**99.13**	**99.34**	**99.51**	**99.4**	**99.25**	**99.69**	**99.14**
Si	1.977	1.979	1.983	1.988	1.972	2.001	1.977	1.974	1.989	1.999
Al	0.023	0.04	0.019	0.015	0.031	0.027	0.042	0.046	0.026	0.022
Cr	0.002	0.003	0.001	0.001	0.002	bdl	0.001	bdl	bdl	bdl
Ti	0.002	0.004	0.005	0.003	0.003	0.002	0.002	0.004	0.003	0.003
Fe^{+3}	bdl	bdl	bdl	bdl	bdl	0.013	bdl	bdl	bdl	0.002
Fe^{+2}	0.399	0.418	0.418	0.442	0.414	0.463	0.48	0.483	0.482	0.478
Mn	0.013	0.017	0.021	0.009	0.011	0.019	0.017	0.021	0.02	0.012
Mg	0.598	0.559	0.607	0.586	0.587	0.539	0.573	0.555	0.558	0.555
Ca	0.974	0.967	0.943	0.954	0.985	0.908	0.898	0.903	0.905	0.903
Na	0.015	0.013	0.011	0.006	0.004	0.014	0.021	0.018	0.02	0.023
K	0.025	0.002	bdl	bdl	0.002	0.007	bdl	0.005	0.004	0.001
Total	4.028	4.002	4.009	4.004	4.011	3.994	4.01	4.011	4.007	3.999
Wo	49.1	49.3	47.4	47.9	49.3	46.7	45.7	46	46.1	46.3
En	30.2	28.5	30.5	29.4	29.4	27.7	29.1	28.3	28.4	28.4
Fs	20.6	22.2	22	22.6	21.2	25.5	25.2	25.7	25.5	25.3
X_{Mg}	**0.6**	**0.57**	**0.59**	**0.57**	**0.59**	**0.54**	**0.54**	**0.53**	**0.54**	**0.54**

Table 5.3 contd. (from calc-silicate granulites)

Sample	**M-7**									
Domain	7	9	12	13	15	17	18	40	43	52
SiO_2	48.93	48.24	48.85	48.52	48.66	47.87	47.59	47.36	47.2	47.98
TiO_2	0.09	0.15	0.12	0.14	0.1	0.11	0.12	0.09	0.08	0.09
Al_2O_3	0.87	0.9	0.8	0.86	0.92	0.75	0.82	0.6	0.82	0.6
Cr_2O_3	0.07	0.07	0.07	0.07	0.08	0.08	0.08	0.07	0.05	0.04
FeO	19.95	21.09	20.57	20.45	20.65	21.68	21.5	20.24	21.48	20.85
MnO	0.31	0.38	0.45	0.18	0.39	0.15	0.28	0.54	0.26	0.35
MgO	5.33	5.15	5.1	5.23	5.06	4.94	4.85	4.89	5.18	5.06
CaO	23.89	23.47	23.13	23.59	23.64	23.44	24.24	24.45	24.04	24.42
Na_2O	bdl	bdl	bdl	bdl	bdl	bdl	bdl	0.13	0.08	0.09
K_2O	bdl	0.02	0.04	0.02	0.04	0.06	0.06	0.02	0.01	0.01
Total	**99.44**	**99.47**	**99.13**	**99.06**	**99.54**	**99.08**	**99.54**	**98.39**	**142.2**	**99.49**
Si	1.956	1.94	1.962	1.951	1.95	1.939	1.925	1.933	1.916	1.936
Al	0.041	0.043	0.038	0.041	0.043	0.036	0.039	0.029	0.039	0.029
Cr	0.002	0.002	0.002	0.002	0.003	0.003	0.003	0.002	0.002	0.001
Ti	0.003	0.005	0.004	0.004	0.003	0.003	0.004	0.003	0.002	0.003
Fe^{+3}	bdl	bdl	bdl	bdl	bdl	bdl	bdl	bdl	bdl	bdl
Fe^{+2}	0.667	0.709	0.691	0.688	0.692	0.735	0.727	0.691	0.729	0.703
Mn	0.01	0.013	0.015	0.006	0.013	0.005	0.01	0.019	0.009	0.012
Mg	0.318	0.309	0.305	0.313	0.302	0.298	0.292	0.297	0.313	0.304
Ca	1.023	1.011	0.996	1.017	1.015	1.018	1.05	1.069	1.046	1.056
Na	bdl	bdl	bdl	bdl	bdl	bdl	bdl	0.01	0.006	0.007
K	bdl	0.001	0.002	0.001	0.002	0.003	0.003	0.001	0.001	bdl
Total	4.02	4.033	4.015	4.023	4.025	4.04	4.052	4.054	4.064	4.05
Wo	50.8	49.7	49.7	50.3	50.3	49.7	50.7	51.7	50.1	51.1
En	15.8	15.2	15.2	15.5	15	14.6	14.1	14.4	15	14.7
Fs	33.5	35.2	35.1	34.2	34.7	35.8	35.1	33.9	34.8	34.2
X_{Mg}	**0.32**	**0.3**	**0.31**	**0.31**	**0.3**	**0.29**	**0.29**	**0.3**	**0.3**	**0.3**

X_{Mg} = Mg/(Fe^{2+}+Mg); bdl = Below Detection Limit

Table 5.4 Chemical analysis and structural formulae (based on 23 Oxygen) of amphibole from maficgranulite and amphibolites.

Sample	**M-13**							**S-9**		
Domain	6-Hbl1	7-Hbl1	9-Hbl2	10-Hbl2	13-Hbl2	14-Hbl2	17-Hbl2	27-c	29-r	40
SiO_2	52.36	51.28	48.15	47.19	48.13	46.68	47.55	47.74	47.38	47.89
TiO_2	0.17	0.35	1.24	1.25	0.91	0.9	1.05	0.59	0.54	0.24
Al_2O_3	2.58	3.69	6.35	5.99	6.17	6.89	6.52	8.65	8.13	8.12
FeO	13.58	13.62	13.29	14.3	14.06	15.85	14.89	14.7	14.08	13.97
MnO	0.33	0.27	0.18	0.26	0.2	0.26	0.22	0.24	0.29	0.29
MgO	14.66	14.03	12.72	12.91	13.33	11.92	12.95	12.25	12.35	13.93
CaO	12.55	12.11	13.04	12.41	12.69	12.02	13.06	11.59	12.08	11.94
Na_2O	0.27	0.44	0.81	0.81	0.71	0.76	0.38	0.88	0.87	0.53
K_2O	0.12	0.23	0.65	0.62	0.49	0.64	0.73	0.3	0.24	0.14
Total	**96.62**	**96.02**	**96.43**	**95.74**	**96.69**	**95.92**	**97.35**	**96.94**	**95.96**	**97.05**
Si	7.68	7.576	7.155	7.08	7.11	7.03	7	7.044	7.05	6.97
Al^{iv}	0.32	0.424	0.845	0.92	0.89	0.97	1	0.956	0.95	1.03
Al^{vi}	0.126	0.218	0.267	0.14	0.19	0.25	0.13	0.548	0.48	0.36
Ti	0.019	0.039	0.139	0.142	0.102	0.102	0.117	0.065	0.06	0.03
Fe^{+3}	0.09	0	0	0.13	0.2	0.17	0.4	0	0	0
Fe^{+2}	1.565	1.682	1.651	1.66	1.54	1.83	1.43	1.814	1.71	1.25
Mn	0.041	0.034	0.023	0.033	0.025	0.033	0.028	0.03	0.037	0.036
Mg	3.206	3.09	2.818	2.898	2.94	2.67	2.84	2.695	2.744	3.02
Ca	1.972	1.917	2.076	2.002	2.01	1.94	2.06	1.832	1.929	1.86
Na	0.077	0.126	0.233	0.236	0.204	0.223	0.109	0.252	0.251	0.151
K	0.022	0.043	0.123	0.119	0.093	0.123	0.138	0.056	0.046	0.026
X_{Mg}	**0.67**	**0.65**	**0.63**	**0.63**	**0.66**	**0.59**	**0.66**	**0.6**	**0.62**	**0.71**

X_{Mg} = Mg/(Fe^{2+}+Mg); Fe^{+3} = (2* Number of oxygen)*(1-(15/cation Total)

Table 5.4 contd. (from amphibolites)

Sample	S-13							S-14		
Domain	27	30	31	34	35	37	38	10	12	17
SiO_2	42.98	43.23	43.67	42.93	42.32	42.95	43.31	42.82	43.09	42.56
TiO_2	1.28	1.19	1.29	1.4	1.43	1.34	1.01	1.4	1.61	1.54
Al_2O_3	10.1	9.95	9.34	10.42	10.61	10.26	9.92	10.53	10.72	10.65
FeO	20.06	19.59	18.59	19.02	19.2	18.71	18.98	20.67	19.85	20.46
MnO	0.4	0.46	0.33	0.28	0.24	0.1	0.42	0.27	0.18	0.22
MgO	8.52	8.69	8.33	8.42	8.19	8.49	8.76	7.1	7.33	7.15
CaO	11.93	11.91	11.84	11.89	11.73	11.92	11.7	11.34	10.92	11.24
Na_2O	1.22	1.26	1.05	1.25	1.22	1.18	1.15	1.14	1.43	1.31
K_2O	0.94	1.01	1	0.94	1.13	1.05	0.99	1.21	1.18	1.25
Total	**97.43**	**97.3**	**95.42**	**96.54**	**96.08**	**96**	**96.23**	**96.48**	**96.31**	**96.38**
Si	6.549	6.594	6.77	6.591	6.548	6.627	6.658	6.633	6.648	6.6
Al^{iv}	1.451	1.406	1.23	1.409	1.452	1.373	1.342	1.367	1.352	1.4
Al^{vi}	0.363	0.383	0.477	0.476	0.483	0.493	0.454	0.556	0.598	0.546
Ti	0.147	0.137	0.15	0.161	0.167	0.156	0.117	0.163	0.187	0.18
Fe^{+3}	0.25	0.18	0	0.054	0.045	0.009	0.118	bdl	bdl	bdl
Fe^{+2}	2.306	2.319	2.41	2.388	2.438	2.406	2.322	2.677	2.561	2.653
Mn	0.051	0.059	0.043	0.036	0.032	0.013	0.055	0.035	0.024	0.029
Mg	1.936	1.976	1.924	1.928	1.89	1.953	2.007	1.639	1.686	1.653
Ca	1.947	1.947	1.966	1.956	1.945	1.971	1.928	1.882	1.805	1.867
Na	0.361	0.373	0.316	0.372	0.367	0.353	0.344	0.343	0.428	0.394
K	0.183	0.197	0.197	0.185	0.224	0.206	0.193	0.238	0.232	0.247
X_{Mg}	**0.46**	**0.46**	**0.44**	**0.45**	**0.44**	**0.45**	**0.46**	**0.38**	**0.4**	**0.38**

bdl = Below Detection Limit ; X_{Mg} = Mg/(Fe^{2+}+Mg); Fe+3 = (2* Number of oxygen)*(1-(15/cation Total)

Table 5.5 Chemical analysis and structural formulae (based on 18 Oxygen) of Cordierite from peliticgranulite.

Sample	**K-1**									
Domain	72	74	75	79	82	83	86	92	93	95
SiO_2	47.86	47.54	48.24	47.58	47.90	48.08	47.1	47.04	47.28	47.45
Al_2O_3	31.38	31.64	32.07	31.13	31.41	31.26	30.67	30.70	30.93	31.17
FeO	8.06	8.25	8.48	7.51	7.29	7.51	7.62	7.76	8.10	7.56
MnO	0.02	0.01	0.12	0.06	0.11	0.05	0.06	0.02	0.01	0.07
MgO	7.85	7.88	7.71	7.86	7.76	7.75	7.48	7.52	7.55	7.6
CaO	0.00	0.05	0.14	0.03	0.00	0.02	0.00	0.01	0.01	0.01
Na_2O	0.46	0.70	0.68	0.76	0.60	0.89	0.83	0.89	0.55	0.87
K_2O	0.06	0.07	0.16	0.09	0.05	0.10	0.07	0.04	0.04	0.06
Total	**95.70**	**96.14**	**97.60**	**95.01**	**95.12**	**95.65**	**93.83**	**93.99**	**94.47**	**94.79**
Si	5.060	5.014	5.025	5.065	5.080	5.082	5.080	5.068	5.070	5.065
Al	3.911	3.934	3.938	3.905	3.927	3.894	3.900	3.899	3.909	3.921
ΣZ	8.971	8.948	8.962	8.970	9.007	8.976	8.980	8.967	8.979	8.986
Fe^{2+}	0.679	0.666	0.701	0.637	0.647	0.637	0.665	0.663	0.705	0.675
Mn	0.002	0.001	0.011	0.005	0.010	0.004	0.005	0.002	0.001	0.006
Mg	1.237	1.239	1.198	1.247	1.227	1.220	1.203	1.208	1.207	1.209
∑Y	1.918	1.906	1.909	1.888	1.883	1.862	1.873	1.873	1.913	1.890
Ca	0.000	0.005	0.015	0.003	0.000	0.002	0.000	0.001	0.001	0.001
Na	0.094	0.143	0.137	0.157	0.123	0.181	0.173	0.186	0.114	0.180
K	0.008	0.009	0.021	0.012	0.007	0.013	0.010	0.005	0.006	0.008
ΣX	0.102	0.157	0.173	0.172	0.130	0.197	0.183	0.192	0.120	0.189
Total	10.991	11.011	11.045	11.030	11.020	11.035	11.035	11.033	11.012	11.070
X_{Mg}	**0.65**	**0.65**	**0.63**	**0.66**	**0.65**	**0.66**	**0.64**	**0.65**	**0.63**	**0.64**

$X_{Mg} = Mg/(Fe^{2+}+Mg)$

Table 5.6 Chemical analysis and structural formulae (based on 22 Oxygen) of biotite from peliticgranulites.

Sample	**K-1**									
Domain	105-c	106-r	108-c	112	115	118	119	121	122	124
SiO_2	34.32	34.47	34.22	34.23	34.76	34.43	34.43	34.53	33.24	34.20
TiO_2	2.61	2.64	3.03	2.54	2.26	3.11	2.69	2.93	3.07	2.85
Al_2O_3	19.06	18.47	18.81	18.94	18.62	18.70	18.92	18.75	19.42	18.46
FeO	23.84	24.96	23.92	24.60	24.16	24.57	24.38	24.22	24.37	25.04
MnO	0.04	bdl	bdl	bdl	0.08	0.03	bdl	bdl	0.01	bdl
MgO	6.26	6.07	5.99	6.24	6.05	6.02	5.96	6.06	6.12	5.94
CaO	bdl	bdl	0.01	bdl	0.00	0.22	0.05	bdl	0.04	0.09
Na_2O	0.20	0.18	0.24	0.20	0.19	0.22	0.24	0.16	0.10	0.17
K2O	8.58	8.81	8.63	8.43	8.53	7.72	8.59	8.17	7.75	8.10
Cl	0.09	0.09	0.11	0.10	0.12	0.13	0.09	0.13	0.05	0.10
F	0.25	0.14	0.21	0.29	0.11	0.00	0.14	0.18	0.02	0.08
Total	**95.25**	**95.83**	**95.17**	**95.57**	**94.88**	**95.15**	**95.49**	**95.13**	**94.19**	**95.03**
Si	5.340	5.360	5.340	5.330	5.429	5.348	5.354	5.373	5.221	5.350
Al^{IV}	2.660	2.640	2.660	2.670	2.571	2.652	2.646	2.627	2.779	2.650
ΣZ	8.000	8.000	8.000	8.000	8.000	8.000	8.000	8.000	8.000	8.000
Al^{VI}	0.840	0.750	0.800	0.810	0.857	0.772	0.822	0.812	0.816	0.754
Ti	0.310	0.310	0.360	0.300	0.265	0.363	0.315	0.343	0.363	0.335
Fe^{2+}	3.100	3.250	3.120	3.200	3.155	3.192	3.170	3.152	3.201	3.276
Mn	0.010	bdl	bdl	bdl	0.011	0.004	bdl	bdl	0.001	bdl
Mg	1.450	1.410	1.390	1.450	1.409	1.394	1.382	1.406	1.433	1.385
ΣX	5.710	5.720	5.670	5.760	5.697	5.725	5.689	5.712	5.814	5.750
Ca	0.000	0.000	0.000	0.000	0.000	0.037	0.008	0.000	0.007	0.015
Na	0.060	0.050	0.070	0.060	0.058	0.066	0.072	0.048	0.030	0.052
K	1.700	1.750	1.720	1.670	1.700	1.530	1.704	1.622	1.553	1.616
ΣY	1.760	1.800	1.790	1.730	1.757	1.633	1.785	1.670	1.590	1.683
Cl	0.020	0.020	0.030	0.030	0.032	0.034	0.024	0.034	0.013	0.027
F	0.120	0.070	0.100	0.140	0.054	0.000	0.069	0.089	0.010	0.025
X_{Mg}	**0.32**	**0.30**	**0.31**	**0.31**	**0.31**	**0.30**	**0.30**	**0.31**	**0.31**	**0.30**

X_{Mg} = Mg/(Fe^{2+}+Mg); bdl = Below Detection Limit

Table 5.6 contd. (from garnet bearing gneisses**)**

Sample	**M-1**									
Domain	13-c	16-r	21-c	22-r	23-c	26-c	27-r	30	37	39
SiO2	34.96	34.88	34.70	34.78	34.12	34.50	34.33	34.78	35.12	34.62
TiO2	3.53	3.44	3.63	3.66	3.41	3.24	2.78	4.23	4.05	3.95
Al2O3	17.75	17.72	17.76	17.78	17.42	17.29	17.76	14.64	14.31	14.18
FeO	20.14	20.51	20.36	21.25	20.90	20.29	21.89	20.37	19.82	20.55
MnO	0.04	0.00	0.00	0.00	0.00	0.00	0.01	0.04	0.02	0.01
MgO	9.11	9.23	9.10	9.07	9.68	9.91	9.93	10.85	10.75	10.23
CaO	0.05	0.11	0.05	0.00	0.05	0.16	0.12	0.18	0.12	0.16
Na2O	0.18	0.15	0.13	0.12	0.12	0.20	0.26	0.43	0.35	0.26
K2O	9.07	8.99	8.83	8.81	8.47	8.22	7.86	8.70	9.12	9.96
Cl	0.01	0.03	0.02	0.02	0.04	0.03	0.02	0.02	0.02	0.02
F	0.32	0.37	0.45	0.31	0.52	0.33	0.32	0.18	0.25	0.16
Total	**95.16**	**95.43**	**95.03**	**95.80**	**94.72**	**94.18**	**95.28**	**94.42**	**93.93**	**94.10**
Si	5.375	5.359	5.351	5.331	5.298	5.352	5.290	5.418	5.497	5.460
AlIV	2.625	2.641	2.649	2.669	2.702	2.648	2.710	2.582	2.503	2.540
ΣZ	8.000	8.000	8.000	8.000	8.000	8.000	8.000	8.000	8.000	8.000
AlVI	0.592	0.567	0.578	0.542	0.486	0.513	0.515	0.106	0.137	0.096
Ti	0.408	0.398	0.421	0.422	0.398	0.378	0.323	0.496	0.477	0.469
Fe^{2+}	2.589	2.635	2.625	2.723	2.714	2.632	2.820	2.653	2.594	2.710
Mn	0.005	bdl	bdl	bdl	bdl	bdl	0.001	0.006	0.003	0.001
Mg	2.088	2.114	2.092	2.072	2.241	2.292	2.281	2.520	2.509	2.405
ΣX	5.683	5.714	5.716	5.760	5.840	5.815	5.941	5.781	5.720	5.682
Ca	0.008	0.018	0.008	bdl	0.008	0.027	0.020	0.030	0.020	0.027
Na	0.054	0.045	0.039	0.036	0.035	0.061	0.078	0.130	0.106	0.080
K	1.779	1.762	1.737	1.722	1.678	1.627	1.545	1.729	1.821	2.004
ΣY	1.841	1.825	1.784	1.758	1.720	1.715	1.643	1.889	1.947	2.110
Cl	0.003	0.008	0.005	0.005	0.011	0.008	0.004	0.004	0.005	0.005
F	0.156	0.180	0.219	0.150	0.254	0.164	0.158	0.089	0.124	0.080
X_{Mg}	**0.45**	**0.45**	**0.44**	**0.43**	**0.45**	**0.47**	**0.45**	**0.49**	**0.49**	**0.47**

X_{Mg} = Mg/(Fe^{2+}+Mg); bdl = Below Detection Limit

Table 5.6 contd. (from mafic granulites**)**

Sample	**M-13**									
Domain	19-c	20-r	24-c	23-r	28	31	34	39	45	47
SiO_2	38.18	37.85	38.45	37.58	38.48	37.61	36.68	38.42	37.83	38.75
TiO_2	4.57	4.49	4.48	4.31	4.25	4.38	4.35	4.18	4.18	4.95
Al_2O_3	14.30	14.17	14.35	14.18	14.61	13.71	13.73	13.74	14.65	14.43
FeO	12.51	12.73	12.66	13.03	13.01	13.98	13.34	13.63	12.93	13.27
MnO	0.17	0.13	0.15	0.16	0.14	0.16	0.13	0.16	0.11	0.14
MgO	15.71	15.48	15.53	15.72	15.74	16.07	16.00	15.23	16.19	15.93
CaO	bdl	bdl	bdl	bdl	bdl	bdl	bdl	bdl	bdl	bdl
Na_2O	0.22	0.21	0.19	0.17	0.18	0.21	0.20	0.17	0.16	0.23
K2O	8.89	8.76	9.08	8.93	8.62	8.52	9.49	9.65	9.43	9.21
Cl	0.08	0.09	0.09	0.09	0.00	0.00	0.00	0.00	0.01	0.03
F	0.53	0.65	0.69	0.47	0.02	0.03	0.01	0.02	0.04	0.01
Total	**95.16**	**94.56**	**95.67**	**94.64**	**95.05**	**94.67**	**93.93**	**95.20**	**95.53**	**96.95**
Si	5.657	5.657	5.680	5.620	5.670	5.611	5.545	5.712	5.583	5.626
Al^{IV}	2.343	2.343	2.320	2.380	2.330	2.389	2.446	2.288	2.417	2.374
ΣZ	8.000	8.000	8.000	8.000	8.000	8.000	7.991	8.000	8.000	8.000
Al^{VI}	0.153	0.153	0.178	0.119	0.207	0.021	0.000	0.120	0.131	0.094
Ti	0.509	0.505	0.498	0.485	0.471	0.491	0.495	0.467	0.464	0.540
Fe^{2+}	1.550	1.591	1.564	1.629	1.603	1.744	1.686	1.694	1.596	1.611
Mn	0.021	0.016	0.019	0.020	0.017	0.020	0.017	0.020	0.014	0.017
Mg	3.470	3.449	3.420	3.505	3.457	3.574	3.606	3.376	3.562	3.448
ΣX	5.704	5.714	5.679	5.758	5.755	5.851	5.803	5.677	5.767	5.711
Ca	bdl	bdl	bdl	bdl	bdl	bdl	bdl	bdl	bdl	bdl
Na	0.063	0.061	0.054	0.049	0.051	0.061	0.059	0.049	0.046	0.065
K	1.680	1.670	1.711	1.703	1.620	1.621	1.830	1.830	1.775	1.706
ΣY	1.743	1.731	1.765	1.753	1.671	1.682	1.888	1.879	1.821	1.770
Cl	0.020	0.022	0.023	0.023	bdl	bdl	bdl	bdl	0.003	0.007
F	0.248	0.307	0.322	0.222	0.009	0.014	0.005	0.009	0.019	0.005
X_{Mg}	**0.69**	**0.68**	**0.69**	**0.68**	**0.68**	**0.67**	**0.68**	**0.67**	**0.69**	**0.68**

X_{Mg} = $Mg/(Fe^{2+}+Mg)$; bdl = Below Detection Limit

Table 5.6 contd. (from amphibolites**)**

Sample	**S-9**					**S-14**				
Domain	18	20	24	26	32	6	9	14	18	19
SiO_2	34.82	34.58	35.18	34.85	34.45	34.80	34.86	34.25	35.74	35.27
TiO_2	2.93	3.74	3.42	3.09	3.17	5.11	4.82	4.85	4.73	4.61
Al_2O_3	15.33	14.68	14.83	14.07	14.13	14.01	14.32	14.65	14.24	14.77
FeO	19.62	19.43	19.62	19.58	19.86	23.73	24.11	23.68	23.44	23.53
MnO	0.09	0.10	0.16	0.14	0.11	0.21	0.16	0.25	0.19	0.19
MgO	11.24	11.57	11.71	11.48	11.53	7.67	7.92	8.62	8.33	8.35
CaO	0.07	bdl	0.01	bdl	0.03	0.03	0.01	0.01	bdl	bdl
Na_2O	0.10	0.03	0.12	0.04	0.11	0.07	0.05	0.03	0.06	0.01
K2O	8.74	8.64	8.95	9.71	9.84	8.98	9.11	8.41	9.40	9.16
Cl	0.07	0.08	0.08	0.06	0.07	0.07	0.06	0.07	0.09	bdl
F	0.63	0.85	0.79	0.56	0.04	0.49	0.43	0.45	0.53	0.03
Total	**95.16**	**94.56**	**95.67**	**94.64**	**94.04**	**95.17**	**95.86**	**95.27**	**96.75**	**95.92**
Si	5.464	5.436	5.465	5.511	5.452	5.492	5.466	5.441	5.534	5.475
Al^{IV}	2.536	2.564	2.535	2.489	2.548	2.508	2.534	2.559	2.466	2.525
ΣZ	8.000	8.000	8.000	8.000	8.000	8.000	8.000	8.000	8.000	8.000
Al^{VI}	0.299	0.156	0.180	0.134	0.087	0.098	0.112	0.125	0.133	0.177
Ti	0.345	0.443	0.400	0.368	0.377	0.606	0.568	0.567	0.551	0.538
Fe^{2+}	2.575	2.555	2.549	2.589	2.628	3.132	3.162	3.078	3.035	3.054
Mn	0.012	0.014	0.021	0.019	0.015	0.029	0.022	0.033	0.025	0.024
Mg	2.629	2.712	2.712	2.707	2.720	1.806	1.851	1.998	1.923	1.932
ΣX	5.861	5.880	5.861	5.816	5.828	5.670	5.714	5.801	5.667	5.727
Ca	0.013	bdl	0.002	bdl	0.005	0.005	0.001	0.002	bdl	bdl
Na	0.031	0.009	0.036	0.012	0.034	0.022	0.017	0.009	0.018	0.003
K	1.750	1.733	1.773	1.960	1.986	1.808	1.822	1.668	1.857	1.814
ΣY	1.793	1.742	1.811	1.972	2.025	1.835	1.839	1.678	1.875	1.817
Cl	0.019	0.020	0.021	0.016	0.020	0.018	0.016	0.018	0.024	bdl
F	0.313	0.423	0.388	0.280	0.020	0.242	0.215	0.221	0.260	0.015
X_{Mg}	**0.51**	**0.52**	**0.53**	**0.52**	**0.51**	**0.37**	**0.37**	**0.39**	**0.39**	**0.39**

X_{Mg} = Mg/(Fe^{2+}+Mg); bdl = Below Detection Limit

Table 5.7 Chemical analysis and structural formulae (based on 8 Oxygen) of Plagioclase from peliticgranulites and garnet bearing gneisses.

Sample	**K-1**					**M-1**				
Domain	91	93	97	98	100	28	29	31	34	35
SiO_2	61.58	61.43	61.14	60.83	62	56.91	56.69	55.62	56.78	62.46
Al_2O_3	23.58	23.48	23.94	23.64	23.28	25.76	26.22	26.44	26.38	21.03
FeO	0.05	0.02	0.03	0.09	0.12	0.11	0.13	0.07	0.15	bdl
CaO	5.41	5.02	5.56	5.1	5.41	8.94	8.94	9.85	9.36	bdl
Na_2O	8.91	8.96	8.67	8.67	8.91	6.7	6.76	6.84	6.36	1.27
K_2O	0.23	0.19	0.21	0.2	0.23	0.16	0.14	0.16	0.03	14.48
Total	**99.76**	**99.1**	**99.55**	**98.53**	**99.95**	**98.58**	**98.88**	**98.98**	**99.06**	**99.24**
Si	2.745	2.752	2.731	2.741	2.758	2.592	2.576	2.538	2.573	2.896
Al	1.239	1.240	1.260	1.256	1.221	1.383	1.404	1.422	1.409	1.149
Fe^{+3}	0.002	0.001	0.001	0.003	0.004	0.004	0.005	0.003	0.006	bdl
Ca	0.258	0.241	0.266	0.246	0.258	0.436	0.435	0.482	0.454	bdl
Na	0.770	0.778	0.751	0.758	0.769	0.592	0.596	0.605	0.559	0.114
K	0.013	0.011	0.012	0.011	0.013	0.009	0.008	0.009	0.002	0.856
Total	5.027	5.012	5.021	5.016	5.023	5.017	5.024	5.058	5.003	5.015
An	0.2	0.2	0.3	0.2	0.2	0.4	0.4	0.4	0.4	bdl
Ab	0.7	0.8	0.7	0.7	0.7	0.6	0.6	0.6	0.6	0.1
Or	bdl	bdl	bdl	bdl	bdl	bdl	bdl	bdl	bdl	0.9

bdl = Below Detection Limit

Table 5.7 contd. (from amphibolites).

Sample	**S-13**					**S-14**				
Domain	19	21	23	24	26	11	13	15	16	18
SiO_2	54.17	55.77	54.49	54.35	54.92	55.25	55.17	54.74	55.28	54.69
Al_2O_3	27.29	28.28	27.65	28.73	28.2	27.68	27.82	26.95	27.31	27.52
FeO	0.22	0.26	0.19	0.12	0.35	0.02	0.21	0.18	0.1	0.02
CaO	10.62	9.55	9.85	9.68	9.28	10.91	11.05	11.18	11.4	11.27
Na_2O	6.58	6.02	6.13	6.46	6.71	5.83	5.24	6.17	5.87	6.03
K_2O	0.16	0.11	0.18	0.21	0.1	0.07	0.06	0.07	0.04	0.08
Total	**99.04**	**99.99**	**98.49**	**99.55**	**99.56**	**99.76**	**99.55**	**99.29**	**100**	**99.61**
Si	2.481	2.508	2.496	2.465	2.489	2.499	2.498	2.498	2.500	2.486
Al	1.474	1.499	1.493	1.536	1.507	1.476	1.485	1.450	1.456	1.474
Fe^{+3}	0.008	0.010	0.007	0.005	0.013	0.001	0.008	0.007	0.004	0.001
Ca	0.521	0.460	0.483	0.470	0.451	0.529	0.536	0.547	0.553	0.549
Na	0.585	0.525	0.544	0.568	0.590	0.511	0.460	0.546	0.515	0.531
K	0.009	0.006	0.011	0.012	0.006	0.004	0.003	0.004	0.002	0.005
Total	5.079	5.008	5.035	5.057	5.055	5.020	4.991	5.052	5.030	5.045
An	0.5	0.5	0.5	0.4	0.4	0.5	0.5	0.5	0.5	0.5
Ab	0.5	0.5	0.5	0.5	0.6	0.5	0.5	0.5	0.5	0.5
Or	bdl	bdl	bdl	bdl	bdl	bdl	bdl	bdl	bdl	bdl

bdl = Below Detection Limit; FeO as Total Iron

Table 5.7 contd. (from amphibolite and mafic granulite).

Sample	**S-9**					**M-13**				
Domain	19	20	21	24	28	25	27	30	33	35
SiO_2	51.14	52.74	52.63	51.93	50.28	55.21	55.49	56.28	56.1	55.66
Al_2O_3	29.74	28.73	28.94	29.26	30.08	27.71	27.82	26.78	26.73	27.44
FeO	0.05	bdl	bdl	bdl	bdl	0.03	0.08	bdl	bdl	0.02
CaO	13.18	11.81	12.19	12.71	12.78	10.74	10.63	9.8	9.89	10.63
Na_2O	4.55	5.03	4.97	4.49	3.78	5.64	5.47	6.17	5.98	5.58
K_2O	0.04	0.05	0.02	0.05	0.77	0.02	0.07	0.15	0.11	0.02
Total	**98.70**	**98.37**	**98.75**	**98.44**	**97.69**	**99.35**	**99.56**	**99.18**	**98.81**	**99.34**
Si	2.358	2.427	2.415	2.393	2.344	2.503	2.508	2.551	2.551	2.521
Al	1.617	1.559	1.565	1.590	1.653	1.481	1.482	1.431	1.433	1.464
Fe^{+3}	0.002	bdl	bdl	bdl	bdl	0.001	0.003	bdl	bdl	0.001
Ca	0.651	0.583	0.600	0.628	0.639	0.522	0.515	0.476	0.482	0.516
Na	0.407	0.449	0.442	0.402	0.341	0.496	0.479	0.542	0.527	0.490
K	0.002	0.003	0.001	0.003	0.046	0.001	0.004	0.009	0.006	0.001
Total	5.038	5.020	5.024	5.014	5.023	5.005	4.992	5.009	4.999	4.993
An	0.6	0.6	0.6	0.6	0.6	0.5	0.5	0.5	0.5	0.5
Ab	0.4	0.4	0.4	0.4	0.3	0.5	0.5	0.5	0.5	0.5
Or	bdl	bdl	bdl	bdl	bdl	bdl	bdl	bdl	bdl	bdl

bdl = Below Detection Limit

Table 5.7 contd. (from calc-silicate granulite).

Sample	**M-7**									
Domain	25	27	30	33	34	36	37	42	44	51
SiO_2	44.08	44.39	44.05	44.68	44.03	44.84	44.74	44.67	43.97	43.28
Al_2O_3	34.36	34.65	34.36	34.11	34.12	33.84	33.72	33.52	34.46	34.85
FeO	0.05	0.14	0.22	0.1	0.27	0.01	0	0	0.01	0.08
CaO	21.1	20.3	20.19	20.67	20.98	20.08	20.28	20.66	20.19	20.55
Na_2O	0.14	0.11	0.81	0.27	0.24	0.62	0.58	0.64	0.72	0.51
K_2O	bdl	0.02	0.17	0.03	0.03	bdl	bdl	0.02	0.07	0.06
Total	**99.73**	**99.61**	**99.8**	**99.86**	**99.67**	**99.39**	**99.32**	**99.51**	**99.42**	**99.33**
Si	2.054	2.064	2.054	2.076	2.056	2.090	2.088	2.085	2.054	2.027
Al	1.887	1.899	1.889	1.868	1.878	1.859	1.855	1.844	1.897	1.924
Fe^{+3}	0.002	0.005	0.009	0.004	0.011	0.000	0.000	0.000	0.000	0.003
Ca	1.053	1.012	1.009	1.029	1.050	1.003	1.014	1.033	1.011	1.031
Na	0.013	0.010	0.073	0.024	0.022	0.056	0.052	0.058	0.065	0.046
K	0.000	0.001	0.010	0.002	0.002	0.000	0.000	0.001	0.004	0.004
Total	5.009	4.992	5.043	5.003	5.017	5.008	5.010	5.022	5.032	5.036
An	1.0	1.0	0.9	1.0	1.0	0.9	1.0	0.9	0.9	1.0
Ab	bdl	bdl	0.1	bdl	bdl	0.1	bdl	0.1	0.1	bdl
Or	bdl	bdl	bdl	bdl	bdl	bdl	bdl	bdl	bdl	bdl

bdl = Below Detection Limit

Table 5.8 Chemical analysis and structural formulae (based on 10 Oxygen) of Sillimanite from peliticgranulites.

Sample	**K-1**									
Domain	73-in	76-mat	77	78	81	87	88	90	94	99
SiO_2	37.15	37.18	37.13	37.28	36.20	36.22	37.05	37.52	37.96	37.83
TiO_2	0.04	bdl	0.05	0.01	0.06	0.03	0.01	0.03	0.01	0.02
Al_2O_3	61.95	61.37	61.55	61.75	62.27	62.72	62.18	60.85	61.06	61.58
Cr_2O_3	0.13	0.03	0.17	0.03	0.08	0.014	0.02	0.04	0.04	0.04
FeO	0.61	0.45	0.99	0.63	0.78	0.58	0.65	0.79	0.86	0.27
Total	99.88	99.03	99.88	99.70	99.39	99.564	99.91	99.24	99.93	99.75
Si	2.021	2.056	2.080	2.110	2.000	2.000	2.100	2.180	2.230	2.210
Ti	bdl	bdl	bdl	bdl	bdl	bdl	bdl	bdl	bdl	bdl
Al	3.953	3.910	3.930	3.950	3.990	4.110	3.990	3.890	3.930	3.940
Cr	0.001	0.001	0.002	0.004	0.008	0.001	0.002	0.004	0.003	0.003
Fe	0.026	0.021	0.040	0.030	0.040	0.020	0.030	0.040	0.040	0.010
Total	6.002	5.988	6.052	6.094	6.038	6.131	6.122	6.114	6.203	6.163

bdl = Below Detection Limit

Table 5.9 Chemical analysis and structural formulae (based on 5 Oxygen) of sphene from calc-silicate granulite (based on 12.5 Oxygen) of clinozoisite and (based on 3 Oxygen) of ilmenite from pelitic granulite, garnet- bearing gneiss andamphibolites.

Sample	**M-7**					**K-1**		**M-1**		**S-9**		**S-14**
Mineral	Sp	Sp	Sp	Sp	Cz	Ilm	Ilm	Ilm	Ilm	Ilm	Ilm	Ilm
Domain	14	16	41	45	6	80	85	36	38	31	42	22
SiO_2	29.2	28.94	30.14	30.17	38.51	0.70	0.60	0.2	0.00	0.07	0.02	0.05
TiO_2	36.5	35.71	35.96	35.57	0.15	51.94	50.59	53.57	51.6	49.58	49.85	43.68
Al_2O_3	2.21	2.33	2.38	2.23	27.62	2.12	2.01	1.14	1.01	0.92	0.85	4.12
Cr_2O_3	0.07	0.01	0.01	0.01	0.04	bdl	bdl	bdl	bdl	bdl	bdl	bdl
FeO	0.58	0.5	0.7	0.28	8.64	43.32	45.02	42.24	45.32	47.12	46.8	49.17
MnO	0.03	bdl	0.12	0.18	0.03	1.41	1.33	0.29	0.76	1.27	1.45	1.46
MgO	0.03	bdl	bdl	bdl	bdl	0.14	0.17	0.39	0.61	0.21	0.38	0.18
CaO	29.8	29.65	29.52	28.7	23.3	0.04	0.07	0.26	0.27	0.14	0.08	bdl
K_2O	0.01	0.02	0.05	0.06	bdl	bdl	0.03	bdl	bdl	bdl	bdl	0.04
Total	**98.5**	**97.16**	**98.88**	**97.2**	**98.29**	**99.68**	**99.82**	**98.09**	**99.57**	**99.31**	**99.43**	**98.70**
Oxygen	5	5	5	5	12.5	3	3	3	3	3	3	3
Si	0.97	0.980	1.000	1.010	2.970	0.035	0.030	0.010	0.000	0.004	0.001	0.002
Ti	0.92	0.910	0.900	0.900	0.010	1.955	1.900	2.059	1.947	1.879	1.886	1.635
Al	0.09	0.090	0.090	0.090	2.510	0.125	0.118	0.069	0.060	0.055	0.050	0.242
Cr	0.01	0.01	0.01	0.01	bdl	bdl	bdl	bdl	bdl	bdl	bdl	bdl
Fe^{+2}	0.02	0.010	0.020	0.010	0.560	1.813	1.879	1.805	1.901	1.985	1.968	2.046
Mn	bdl	bdl	bdl	0.010	bdl	0.060	0.056	0.013	0.032	0.054	0.062	0.062
Mg	bdl	bdl	bdl	bdl	bdl	0.010	0.013	0.030	0.046	0.016	0.028	0.014
Ca	1.07	1.070	1.050	1.030	1.920	0.002	0.003	0.014	0.015	0.008	0.004	0.000
K	0.00	0.002	0.005	0.006	bdl	0.000	0.003	0.000	0.000	0.000	0.000	0.004
Total	3.06	3.070	3.060	3.050	8.010	4.000	4.003	4.000	4.000	4.000	4.000	4.004

bdl = Below Detection Limit

Table 5.10 Representative electron microprobe analyses (EPMA), structural formula with their associated age of monazitegrains (based on 4 Oxygens).

Sample	**K1/1**	**K1/3**	**K1/5**	**K1/7**	**K1/8**	**K1/9**	**K1/10**	**K1/11**	**K1/12**	**K1/13**	**K1/14**	**K1/15**	**K1/16**	**K1/17**
SiO2	0.57	0.42	0.56	0.51	0.76	0.52	0.71	2.13	3.26	0.61	0.54	0.71	0.71	5.64
P2O5	28.39	28.76	30.73	30.42	30.02	30.54	30.16	27.14	29.22	28.97	30.77	29.26	28.58	29.71
CaO	3.58	4.34	1.40	0.95	0.97	0.99	0.96	1.54	0.57	1.45	1.47	1.47	1.48	1.23
Y2O3	0.94	0.58	0.23	0.69	0.63	0.78	0.63	2.22	0.26	bdl	bdl	0.09	bdl	bdl
La2O3	13.48	14.55	15.01	16.27	15.70	16.10	15.70	17.02	17.76	17.28	15.05	13.53	14.82	14.03
Ce2O3	27.19	27.29	28.48	28.90	28.54	28.73	29.68	25.82	25.19	27.16	27.83	28.49	28.12	27.50
Pr2O3	3.10	3.07	3.24	3.04	3.01	3.09	3.04	2.16	2.19	2.85	3.06	3.09	3.04	2.73
Nd2O3	9.90	10.04	10.23	9.73	9.62	10.01	9.58	6.15	5.47	9.72	9.87	10.56	11.17	9.30
Sm2O3	1.55	1.41	1.44	1.25	1.24	1.07	1.23	0.65	0.71	1.35	1.58	1.58	1.56	0.79
Eu2O3	bdl	bdl	bdl	bdl	bdl	bdl	bdl	bdl	bdl	bdl	bdl	bdl	bdl	bdl
Gd2O3	0.94	0.43	0.67	0.65	0.78	0.59	0.58	0.54	0.39	0.53	0.58	0.78	0.73	0.52
PbO	0.67	0.57	0.56	0.43	0.52	0.45	0.50	1.04	1.07	0.61	0.61	0.68	0.68	0.54
ThO2	7.34	6.85	6.55	5.31	6.65	5.68	6.01	12.00	11.86	7.70	8.01	8.63	8.43	6.72
UO2	0.52	0.28	0.22	0.12	0.18	0.12	0.15	0.62	0.73	0.21	0.31	0.02	0.25	0.24
Total	**98.17**	**98.59**	**99.30**	**98.27**	**98.61**	**98.67**	**98.92**	**99.01**	**99.69**	**98.43**	**99.67**	**98.90**	**99.56**	**98.96**
Si	0.023	0.017	0.022	0.02	0.03	0.02	0.03	0.086	0.126	0.024	0.021	0.028	0.028	0.207
P	0.96	0.962	0.995	1.008	0.997	1.008	1.00	0.923	0.956	0.98	1.008	0.982	0.967	0.925
Ca	0.153	0.184	0.059	0.04	0.041	0.041	0.04	0.066	0.024	0.062	0.061	0.063	0.063	0.048
Y	0.018	0.011	0.004	0.013	0.012	0.014	0.011	0.042	0.005	bdl	bdl	0.002	bdl	bdl
La	0.199	0.212	0.219	0.235	0.227	0.231	0.226	0.252	0.253	0.255	0.215	0.198	0.218	0.19
Ce	0.398	0.395	0.412	0.414	0.41	0.41	0.425	0.379	0.356	0.398	0.394	0.414	0.411	0.37
Pr	0.045	0.044	0.047	0.043	0.043	0.044	0.043	0.032	0.031	0.041	0.043	0.045	0.044	0.037
Nd	0.141	0.142	0.144	0.136	0.135	0.139	0.134	0.088	0.076	0.139	0.136	0.15	0.159	0.122
Sm	0.021	0.019	0.02	0.017	0.017	0.014	0.017	0.009	0.009	0.019	0.021	0.022	0.021	0.01
Eu	bdl	bdl	bdl	bdl	bdl	bdl	bdl	bdl	bdl	bdl	bdl	bdl	bdl	bdl
Gd	0.012	0.006	0.009	0.008	0.01	0.008	0.008	0.007	0.005	0.007	0.007	0.01	0.01	0.006
Pb	0.007	0.006	0.006	0.005	0.005	0.005	0.005	0.011	0.011	0.007	0.006	0.007	0.007	0.005
Th	0.067	0.062	0.059	0.047	0.059	0.05	0.053	0.11	0.104	0.07	0.07	0.078	0.077	0.056
U	0.005	0.002	0.002	0.001	0.002	0.001	0.001	0.006	0.006	0.002	0.003	0.002	0.002	0.002
Total	2.049	2.061	1.998	1.987	1.987	1.986	1.989	2.01	1.962	2.004	1.986	1.999	2.01	1.98
Age (Ma)	**1650**	**1654**	**1743**	**1719**	**1616**	**1661**	**1735**	**1667**	**1687**	**1639**	**1529**	**1633**	**1659**	**1636**
Age err	**47**	**52**	**57**	**68**	**56**	**64**	**62**	**39**	**38**	**50**	**47**	**48**	**48**	**53**

Weighted mean age 1655 ± 30 Ma (n = 14, MSWD = 4.3); bdl = Below Detection Limit

Contd. (Pelitic granulites and garnet bearing gneisses)

Sample	**K1/2**	**K1/4**	**K1/6**	**M1/1**	**M1/2**	**M1/3**	**M1/4**	**M1/5**	**M1/6**	**M1/7**	**M1/8**
SiO2	5.16	7.84	20.81	0.42	0.61	0.21	0.36	0.35	0.3	1.01	0.35
P2O5	28.41	28.33	28.41	30.6	32.14	31.05	30.84	31.06	30.9	30.48	30.15
CaO	6.15	1.61	1.74	1.36	1.7	1.4	1.45	1.47	1.54	1.51	1.33
Y2O3	0.65	0.55	0	2.19	2.15	1.62	1.77	1.8	1.65	2.48	1.71
La2O3	15.74	15.74	8.27	14.69	13.67	13.72	13.15	13.52	13.08	13.24	13.86
Ce2O3	27.88	27.92	5.32	28.8	26.27	28.58	28.43	28.24	27.14	28.38	28.54
Pr2O3	2.95	2.12	bdl	2.32	2.64	2.95	2.5	2.74	2.87	2.86	2.85
Nd2O3	6.49	10.87	bdl	9.12	9.22	9.55	10.27	10.29	9.11	8.99	10.44
Sm2O3	bdl	0.31	bdl	0.2	1.7	1.84	1.75	1.86	1.82	1.68	1.84
Eu2O3	bdl	bdl	bdl	bdl	bdl	bdl	bdl	bdl	bdl	bdl	bdl
Gd2O3	0.74	0.53	bdl	0.43	1.4	1.36	1.41	1.41	1.62	1.48	1.57
PbO	0.16	0.19	0.21	bdl	0.35	0.45	0.36	0.37	0.61	0.31	0.32
ThO2	3.6	3.16	4.49	9.03	5.53	6.25	6.82	6.26	6.33	6.18	6.17
UO2	0.2	0.23	0.17	0.3	0.91	0.7	0.75	0.62	1.05	0.82	0.68
Total	**98.13**	**99.17**	**100.48**	**99.44**	**98.28**	**99.7**	**99.84**	**99.98**	**98.02**	**99.4**	**99.79**
Si	0.19	0.283	0.735	0.016	0.023	0.008	0.014	0.014	0.012	0.039	0.014
P	0.885	0.866	0.849	1.003	1.031	1.014	1.009	1.01	1.019	0.992	0.996
Ca	0.242	0.062	0.066	0.056	0.069	0.058	0.06	0.061	0.064	0.062	0.056
Y	0.011	0.009	0	0.04	0.038	0.029	0.032	0.032	0.03	0.045	0.031
La	0.214	0.21	0.108	0.21	0.191	0.195	0.19	0.191	0.188	0.188	0.199
Ce	0.376	0.369	0.069	0.408	0.364	0.404	0.398	0.397	0.387	0.399	0.407
Pr	0.04	0.028	bdl	0.033	0.036	0.042	0.035	0.038	0.041	0.04	0.041
Nd	0.085	0.14	bdl	0.126	0.125	0.132	0.14	0.141	0.127	0.123	0.145
Sm	bdl	0.004	bdl	0.003	0.022	0.024	0.023	0.025	0.024	0.022	0.025
Eu	bdl	bdl	bdl	bdl	bdl	bdl	bdl	bdl	bdl	bdl	bdl
Gd	0.009	0.006	bdl	0.006	0.018	0.017	0.018	0.018	0.021	0.019	0.02
Pb	0.002	0.002	0.002	0	0.004	0.005	0.004	0.004	0.006	0.003	0.003
Th	0.03	0.026	0.036	0.08	0.048	0.055	0.059	0.055	0.056	0.054	0.055
U	0.002	0.002	0.001	0.003	0.008	0.006	0.006	0.005	0.009	0.007	0.006
Total	2.084	2.007	1.866	1.984	1.977	1.989	1.989	1.991	1.985	1.994	1.998
Age (Ma)	**874**	**1011**	**969**	**889**	**936**	**1003**	**885**	**1014**	**991**	**822**	**874**
Error	**65**	**74**	**60**	**48**	**38**	**42**	**36**	**41**	**43**	**36**	**38**

Weighted mean age 910 ± 31 Ma (n = 19, MSWD = 9.3); bdl= Below Detection Limit

Contd. (garnet bearing gneisses)

Sample	**M1/9**	**M1/10**	**M1/11**	**M1/12**	**M1/13**	**M1/14**	**M1/15**	**M1/16**
SiO2	0.37	0.34	0.43	1.81	0.35	0.46	0.23	9.04
P2O5	30.29	30.16	30.08	28.21	29.91	30.32	30.69	30.24
CaO	1.41	1.52	1.55	1.40	1.54	1.38	1.47	1.71
Y2O3	1.64	2.60	1.87	2.56	2.59	2.66	2.71	0.93
La2O3	13.94	13.49	13.56	13.33	13.48	13.18	14.39	12.04
Ce2O3	27.58	28.34	28.42	27.98	28.40	27.59	28.10	27.69
Pr2O3	2.70	2.79	2.97	2.87	2.85	2.63	2.68	1.44
Nd2O3	10.21	9.04	9.57	9.37	9.26	8.86	9.35	8.59
Sm2O3	1.74	1.53	1.95	1.73	1.76	1.64	1.13	0.61
Eu2O3	bdl	bdl	bdl	bdl	bdl	bdl	bdl	bdl
Gd2O3	1.39	1.41	1.49	1.72	1.50	1.61	1.51	0.48
PbO	0.34	0.34	0.33	0.32	0.36	0.34	0.57	0.29
ThO2	6.51	6.84	6.37	6.12	6.76	6.60	5.86	4.92
UO2	0.71	0.73	0.66	0.72	0.71	0.79	0.69	0.64
Total	**98.83**	**99.13**	**99.24**	**98.13**	**99.46**	**98.07**	**99.36**	**98.61**
Si	0.014	0.013	0.017	0.072	0.014	0.018	0.009	0.315
P	1.003	0.997	0.995	0.947	0.991	1.005	1.007	0.891
Ca	0.059	0.064	0.065	0.060	0.064	0.058	0.061	0.064
Y	0.030	0.048	0.034	0.048	0.048	0.049	0.049	0.015
La	0.201	0.194	0.195	0.195	0.195	0.190	0.206	0.154
Ce	0.395	0.405	0.407	0.406	0.407	0.395	0.399	0.353
Pr	0.038	0.040	0.042	0.041	0.041	0.038	0.038	0.018
Nd	0.143	0.126	0.133	0.133	0.129	0.124	0.129	0.107
Sm	0.023	0.021	0.026	0.024	0.024	0.022	0.015	0.007
Eu	bdl	bdl	bdl	bdl	bdl	bdl	bdl	bdl
Gd	0.018	0.018	0.019	0.023	0.019	0.021	0.019	0.006
Pb	0.004	0.004	0.003	0.003	0.004	0.004	0.006	0.003
Th	0.058	0.061	0.057	0.055	0.060	0.059	0.052	0.039
U	0.006	0.006	0.006	0.006	0.006	0.007	0.006	0.005
Total	1.993	1.997	2.000	2.012	2.002	1.989	1.996	1.976
Age (Ma)	**886**	**850**	**886**	**865**	**908**	**862**	**994**	**955**
Error	**37**	**36**	**38**	**38**	**37**	**35**	**52**	**45**

Weighted mean age 910 ± 31 Ma (n = 19, MSWD = 9.3); bdl= Below Detection Limit